Tethering Three Radical Cascades for Controlled Termination of Radical Alkyne *peri*-Annulations: Making Phenalenyl Ketones without Oxidants

Chaowei Hu,[†] Leah Kuhn,[†] Favour D. Makurvet,[†] Erica S. Knorr,[†] Xinsong Lin,[†] Rahul K. Kawade,[†] Frederic Mentink-Vigier,[‡] Kenneth Hanson,[†] Igor V. Alabugin[†]*

†: Florida State University, Department of Chemistry and Biochemistry, Tallahassee, FL, 32306-4390, United States. E-mail: alabugin@chem.fsu.edu
‡: National High Magnetic Field Laboratory, Florida State University, Tallahassee, FL, 32310, United States.

Abstract: Although Bu_3Sn-mediated radical alkyne *peri*-annulations allow access to phenalenyl ring systems, the oxidative termination of these cascades provides only a limited selection of the possible isomeric phenalenone products with product selectivity controlled by the intrinsic properties of the new cyclic systems. In this work, we report an oxidant-free termination strategy that can overcome this limitation and enable selective access to the full set of isomeric functionalized phenalenones. The key to preferential termination is preinstallation of "a weak link" that undergoes C-O fragmentation in the final cascade step. Breaking a C-O bond is assisted by entropy, gain of conjugation in the product, and the release of stabilized radical fragments. This strategy is expanded to radical *exo-dig* cyclization cascades of oligoalkynes which open access to isomeric π-extended phenalenones. Conveniently, these cascades introduce functionalities (i.e., Bu_3Sn and iodide moieties) amenable to further cross-coupling reactions. Consequently, variety of polyaromatic diones, which could serve as phenalenyl-based open-shell precursors, can be synthesized.

INTRODUCTION

Of the three possible fusions of three benzene rings, phenalenyl is the most unusual. Unlike anthracene and phenanthrene, which are common stable molecules readily available from many commercial-sources, phenalenyl has an odd number of carbons and, hence, *has to* have an odd number of electrons, i.e., be a radical (Figure 1). The non-Kekulé structure with an odd number of carbons accounts for many interesting properties of phenalenyls[1–14] and a special role of this polycyclic fusion as the prototype building block for the design and synthesis of larger conjugated spin systems.[15–18] Furthermore, the unusual electronic structure of phenalenyl leads to interesting photophysics,[19,20] intriguing magnetic behavior,[21–23] useful amphoteric redox properties[24–29] and applications in catalysis.[30–35]

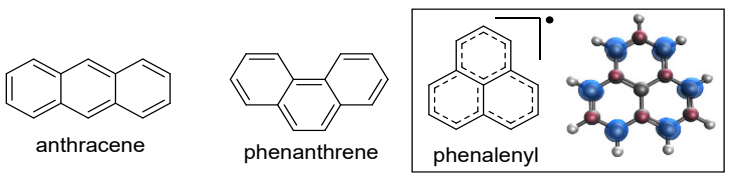

Figure 1. The three possible fusions of three benzene rings and the unusual electronic structure of phenalenyl.

However, preparation of phenalenyls is challenging and they are generally generated *in situ*. In particular, the respective ketones (phenalenones) can serve as convenient precursors for phenalenyls as a sequence of nucleophilic addition to polycyclic ketones followed by *in situ* deoxygenation, which is a useful strategy toward functionalized polyaromatic molecules with interesting properties (e.g. open-shell molecules) (Figure 2).[36–79] For example, Anthony used this approach to prepare silylethynyl functionalized pentacenes[80] while Arikawa and coworkers synthesized triangulene.[81] Our group recently utilized polyaromatic diones to synthesize Kekulé and non-Kekulé diradicaloids with very low singlet/triplet gaps.[82]

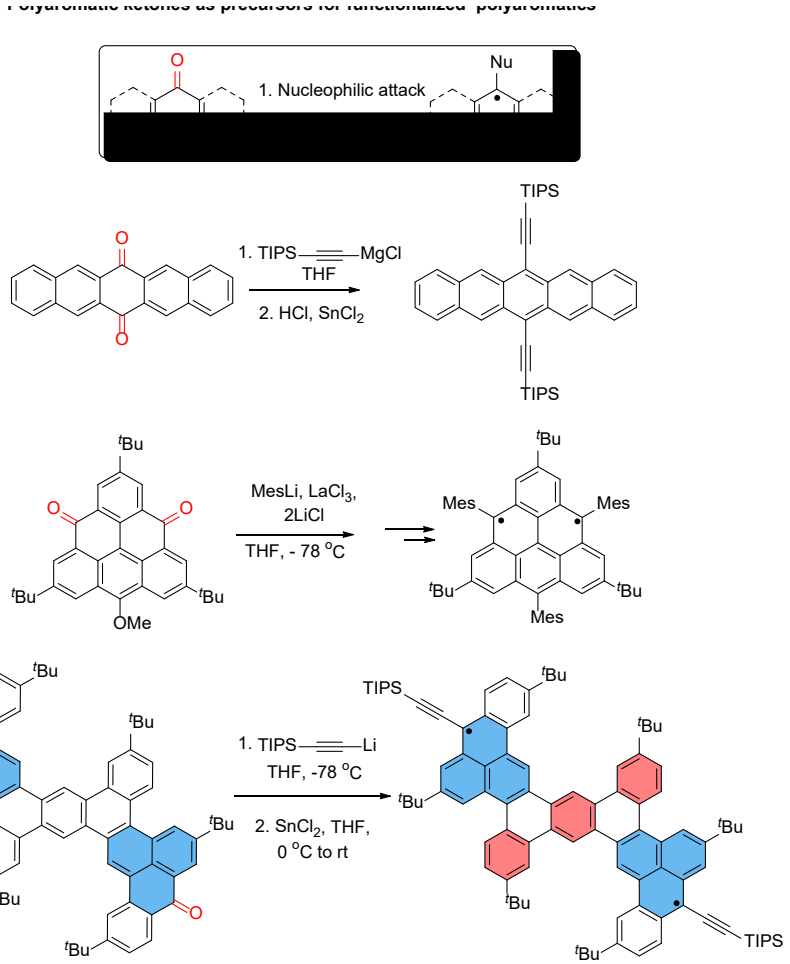

Figure 2. Polyaromatic ketones as precursors for extended polyaromatics.[80–82]

Previously we reported a modular synthetic approach to phenalenyl ketones and their expanded analogs by radical *peri*-annulations of alkynes[83] that take advantage of the carbon-rich nature and high energy content of this functional group.[84–97] The *peri*-annulations are a promising a strategy for expanding the zigzag edge of carbon nanostructures.[83,98] Whereas double *peri*-annulation allows full aromatization by elimination of MeOH, analogous termination of single *peri*-annulations forms a phenalenyl radical, which, due to its instability associated with the open-shell structure, requires an additional step for conversion into a stable product (Scheme 1). Termination of a *single peri*-annulation by oxidation or reduction gives, respectively, either polycyclic ketones or partially reduced aromatic hydrocarbons (Scheme 1).[83] Not only are the ketone products useful precursors for the preparation of new carbon rich molecules, as discussed above, but they have been also explored for the design of lithium-ion batteries.[99]

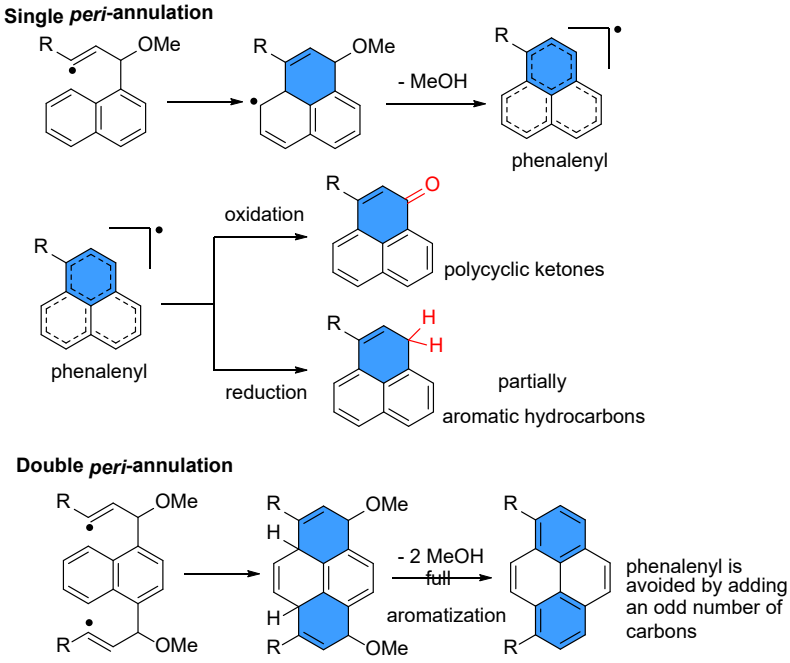

Scheme 1. Comparison of termination strategies for single and double *peri*-annulations.

However, synthesis of such ketones has two limitations: 1) an oxidant is required and 2) selectivity for the formation of isomeric ketones cannot be controlled. As a result, all but one of the five isomeric ketones were previously inaccessible (Figure 3). Only one product was produced in a modest (38%) yield with trace amount of another isomeric ketone. Considering the need for all five isomeric ketones for our future explorations of phenylenyl radicals, we were interested in finding a general synthetic solution to such a problem.

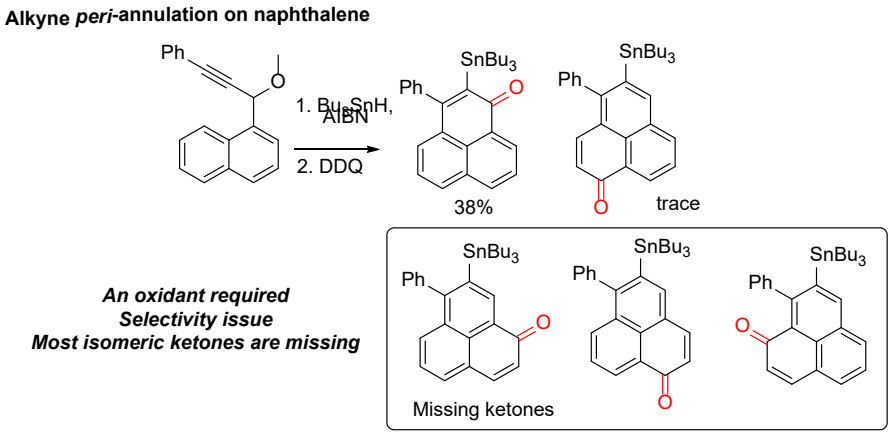

Figure 3. Oxidative termination of alkyne *peri*-annulation with naphthalene provides access to one of five possible isomeric phenalenones.

Here, we take advantage of a C-O radical fragmentation strategy to address these limitations. Due to the relatively high thermodynamic stability of the carbonyl moiety,[100] radical fragmentation with the formation of a carbonyl group is a useful synthetic transformation (Figure 4a). Such transformations can

proceed via fragmentations of either a C-O bond or a C-C bond and have found two notable applications: a) to generate radical species[101–108] or b) to make ketones.[109–115] In the first of these applications, the carbonyl group is the by-product while, in the second type of applications, it is the target.

Many interesting examples of both fragmentation types can be found in the literature (Figure 4b). The utility of these reactions correlates with the stability of carbonyl derivatives. Not surprisingly, loss of CO_2 from the corresponding RCO_2[107] or O=COR[116] radicals are highly favorable and useful for generating carbon-centered radicals, •R. In the classic Barton–McCombie deoxygenation reaction, C-O bond fragmentation generates a C-radical with the help of thioester formation.[117] Our group repurposed this classic reaction by using O → C transpositions to convert phenols into benzoates and terminating the cascade by a fragmentation that forms an ester moeity.[118] The lactone formation after the interception of the p-benzene product of Bergman cyclization was used to transpose one of the radical centers and prevent retro-Bergman ring opening.[119] MacMillan and Doyle groups achieved deoxygenative cross-couplings of alcohols[120,121] and methylation of (hetero)aryl chloride,[122] respectively, by making radical species through C-O bond fragmentations with the formation of highly stabilized carbonyl groups in the carbamate and carbonate by-products.

(a) Carbonyl formation by radical fragmentation: C-C vs. C-O fragmentation

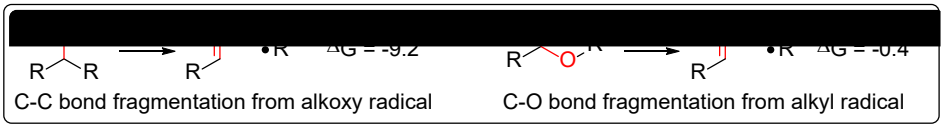

(b) Literature examples of carbonyl formation by radical fragmentation

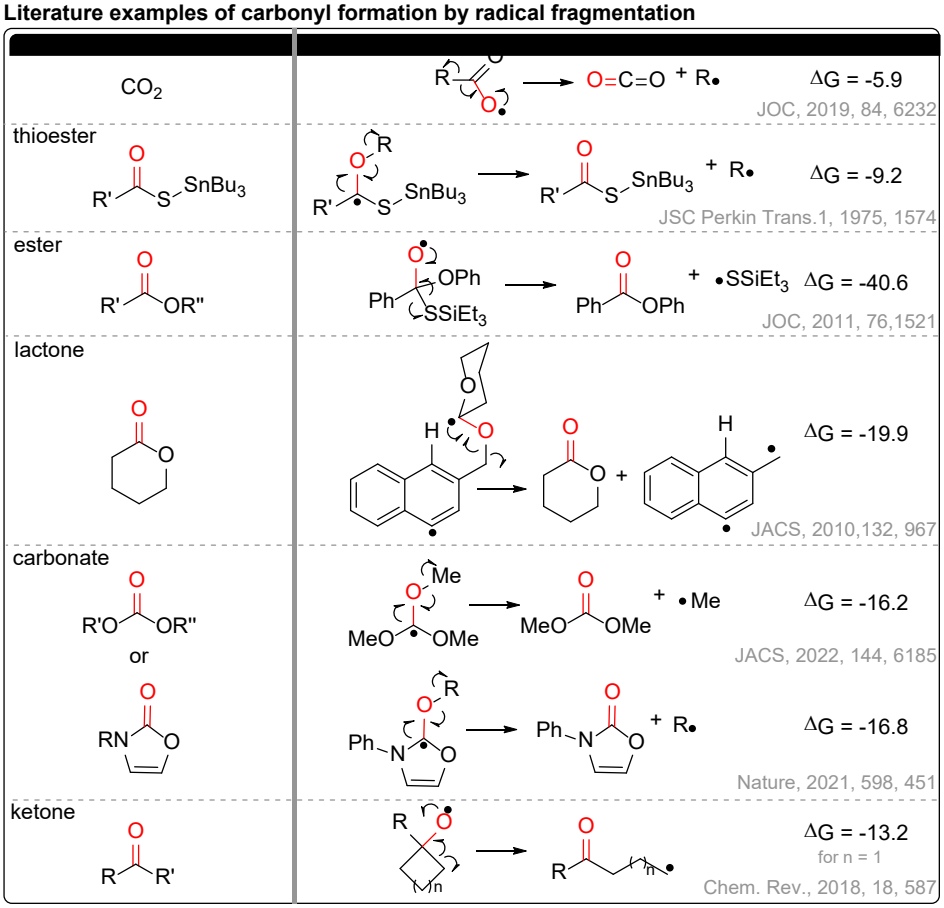

free energies in kcal/mol, all R-groups = CH_3

Figure 4. (a) Carbonyl formation by radical fragmentation. (b) Literature examples of exergonic carbonyl formation by radical fragmentation.

The formation of ketones receives less thermodynamic assistance than formation of CO_2, XC(O)Y and RC(O)X derivatives[100] but is still viable. Figure 4b illustrates the difference between the two possible approaches: C-C scission in an O-centered radical or C-O scission in a C-centered radical. Although the formation of a relatively unstable methyl radical is thermodynamically viable in both cases, the C-C bond scission is quite exergonic (ΔG = -9 kcal/mol) while C-O scission is only favorable due to the entropic assistance to fragmentation (ΔG = -0.4 kcal/mol).

Not surprisingly, formation of alkoxy radicals has been used for carbonyl formation quite often.[123–125] In particular, alkoxy radicals derived from cycloalkanols along with C-C bond fragmentation can make ketone products (Figure 4b).[126,127] On the other hand, C-O fragmentations are less common. An interesting example of the latter is formation of polymeric ketones in radical ring-opening polymerization of cyclic vinyl ethers. The intermediate after radical addition to the alkene undergoes ring-opening by C-O bond cleavage, giving an alkyl radical that continues polymerization.[128,129]

Encouraged by the known carbonyl-forming C-O fragmentations, we sought to develop an efficient and selective route to functionalized isomeric phenylphenalenones and π-extended phenalenone derivatives by radical alkyne *peri*-annulations terminated by C-O fragmentation. This strategy introduces a C-O bond in the early stage of the syntheses so that the oxidized polyaromatics are prepared without oxidative workup.

Phenylphenalenyl radical is highly delocalized, with six perimeter carbons sharing spin density (Scheme 2a). The radical *peri*-cyclization creates the phenalenyl framework with two substituents at one of the rings while the other two rings have no substituents (Scheme 2b). Four carbons at the two unsubstituted rings have significant spin density that can potentially be used as a target for subsequent reactions. This delocalization of spin density complicates control of regioselectivity for the subsequent trapping of this intermediate under oxidative condition and potentially leads to mixtures of ketone products.

In our work, single isomeric polyaromatic ketones can be formed selectively by C-O radical fragmentation. Although introduction of the O-containing leaving group does not greatly change the spin density (Figure S15), the following C-O radical fragmentation can “capture” each of the four resonance structures to selectively form each of the four isomeric π-extended phenalenones without the need for additional oxidative workup (Scheme 2b).

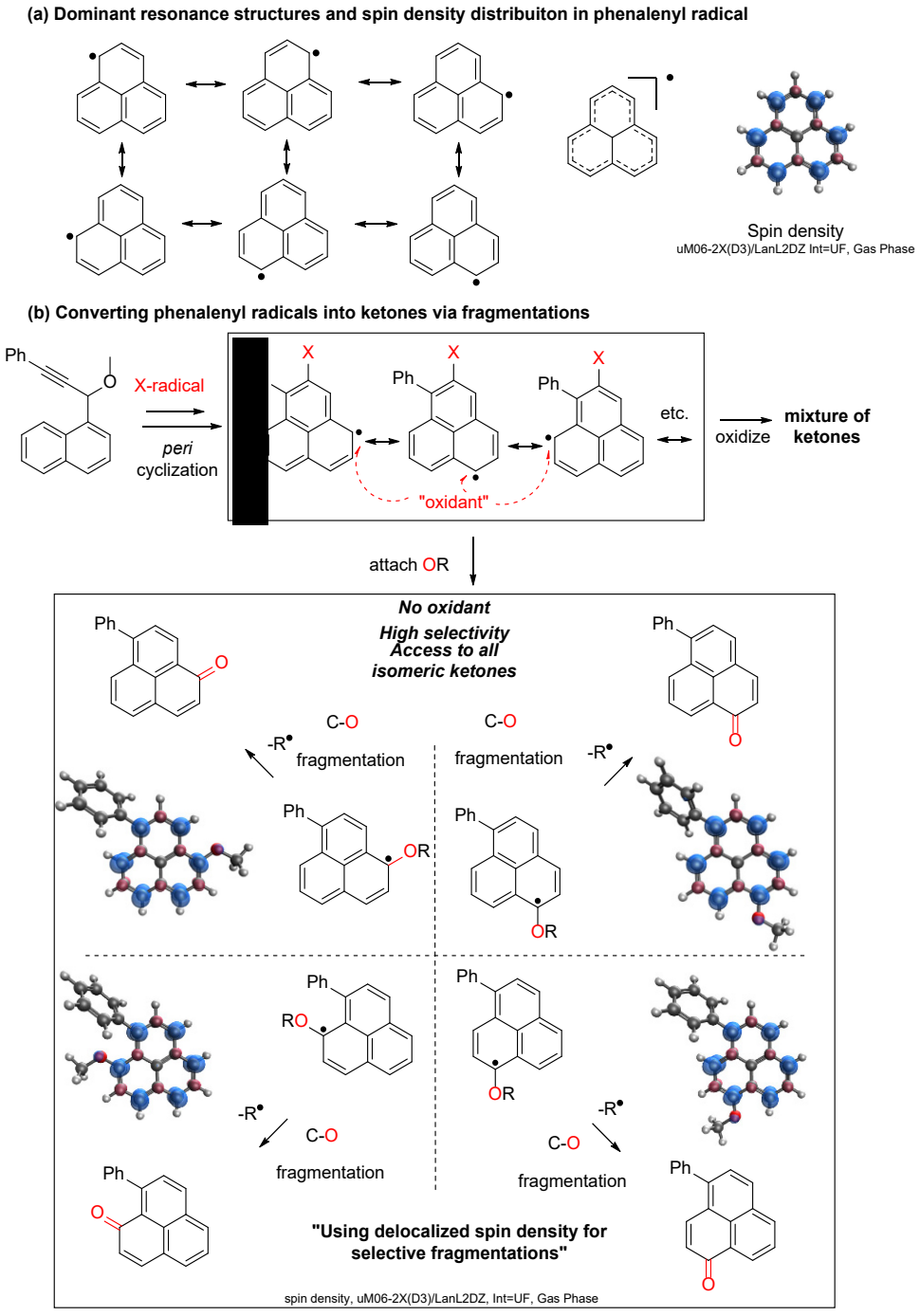

Scheme 2. (a) Dominant resonance structures and spin density distribuiton in phenalenyl radical. (b) "Capturing spin density" at different positions of delocalized phenalenyl radical via fragmentations.

RESULTS AND DISCUSSION

We started the exploration of directed *peri*-annulations with the naphthalene system as it provides access to the parent phenalenyl skeleton. The naphthalenyl benzyl ether derivative **1** was prepared from 2-hydroxynaphthaldehyde in two steps (See SI). The usual conditions for the radical chain reactions[130,131] (i.e., the catalytic amount of AIBN (0.2 equiv) and slight excess (1.3 equiv) of radical

precursor Bu_3SnH (Table *1*, entry 1) gave mostly unreacted starting material with only trace amounts of the desired phenalenone. An attempt to increase the propagation efficiency by using thiophenol as a polarity-reversal catalysis was unsuccessful (Table *1*, entry 2). On the other hand, an increase in the amount of initiator of the radical source resulted in higher conversion and increased yield of the desired product (Table *1*, entry 3-5). However, addition of more than one molar equivalent of the initiator became counterproductive (Table *1*, entry 6). After screening different radical sources, initiators, solvents, and initial concentrations of starting material (Table *1*, entry 10-12 and SI), the best yield was obtained with 0.04 M starting material, two equivalents Bu_3SnH (0.3 M) and one equivalent AIBN (0.15 M) in refluxing toluene. Note that equivalent of AIBN should generate two equivalents of C-centered radicals. The need to use a large amount of AIBN suggests the inefficiency of the radical propagation, which is consistent with the multiple roles of AIBN,[132] which can be involved in more than one step of the radical cascade (See SI). Oxidative workup with DDQ did not increase the yield (Table *1*, entry 8).

With these results, we explored the leaving group effect on this transformation. First, we tested whether we could facilitate the C-O bond fragmentation by stabilizing the departing radical either by an oxygen atom or by a phenyl substituent. However, substrate with a methoxymethyl substituent didn't undergo the fragmentation step (Table *1*, entry 14), which indicates that radical stabilization provided by an oxygen atom is insufficient. Substrate with a diphenyl methyl leaving group gave a 36% yield of product (Table *1*, entry 13). However, the starting material was not fully converted even though two phenyl groups should provide greater stabilization to the departing radical. This behavior is likely to stem from the steric hindrance of the substituents. In the end, the benzyl group turned out to be the best leaving group presumably because the single phenyl moiety doesn't hinder the intramolecular initiation step but can still sufficiently stabilize the departing benzylic radical.

Table 1. Optimization of radical cyclization.

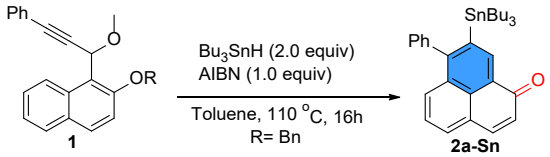

Entry	Deviation from the above reaction	Yield (% conversion)
1	Bu_3SnH (1.3 equiv)/AIBN (0.2 equiv)	Trace
2	Bu_3SnH (1.3 equiv), AIBN (0.2 equiv), PhSH(0.2 equiv)	Trace
3	AIBN (0.5 equiv)	6% (37%)
4	AIBN (0.8 equiv)	30% (83%)
5	None	53% (100%)
6	AIBN (1.2 equiv)	44% (100%)
7	Bu_3SnH (1.5 equiv)	37% (86%)
8	with DDQ workup	29%[a] (100%)
9	Benzene, 80 °C	38% (64%)
10	ABCN (1.0 equiv)	26% (74%)
11	Et_3SiH (2.0 equiv)	0%[a] (74%)
12	Ph_3SnH (2.0 equiv)	39%[a] (100%)
13	R = $CHPh_2$	36% (88%)
14	R = CH_2OMe (MOM)	0%[b](100%)
15	No radical source and initiator	0% (0%)

Initial radical source concentration: 0.3 M. Initial initiator concentration: 0.15 M. Initial starting material concentration: 0.04 M.
[a]NMR yield based on internal standard: 1,2-dichloroethane. [b]complex mixture of products.

With optimized conditions in hand, we tested the scope of the reaction by preparing a series of disubstituted phenalenones. Although the yields were moderate (7-42%), the reaction is tolerant of both electron-donating and electron-withdrawing aryl groups as well as alkyl substituents. The electron-donating groups gave lower yields, possibly due to the lower electrophilicity of the vinyl radical intermediates.[133] Alkyl substituents have the lowest yield among this series, likely because the alkyl substituted vinyl radical are less stable than the aryl substituted analogs.

Gratifyingly, the method provides access to all positional isomeric substituted phenalenones, including 4-, 6-, and 9-phenylphenalenones that were synthesized selectively without the oxidative workup (Figure 5). For each isomeric phenalenone, alkyl substituents, electron-donating groups, and electron-withdrawing groups are also tolerated. The yields trend follows the relative stability of the phenalenones. 9-Substituted phenalenones gave the lowest yields probably due to the unfavorable sterics in the product. In some cases, iodination was performed if isolation of the pure stannylated products was difficult.

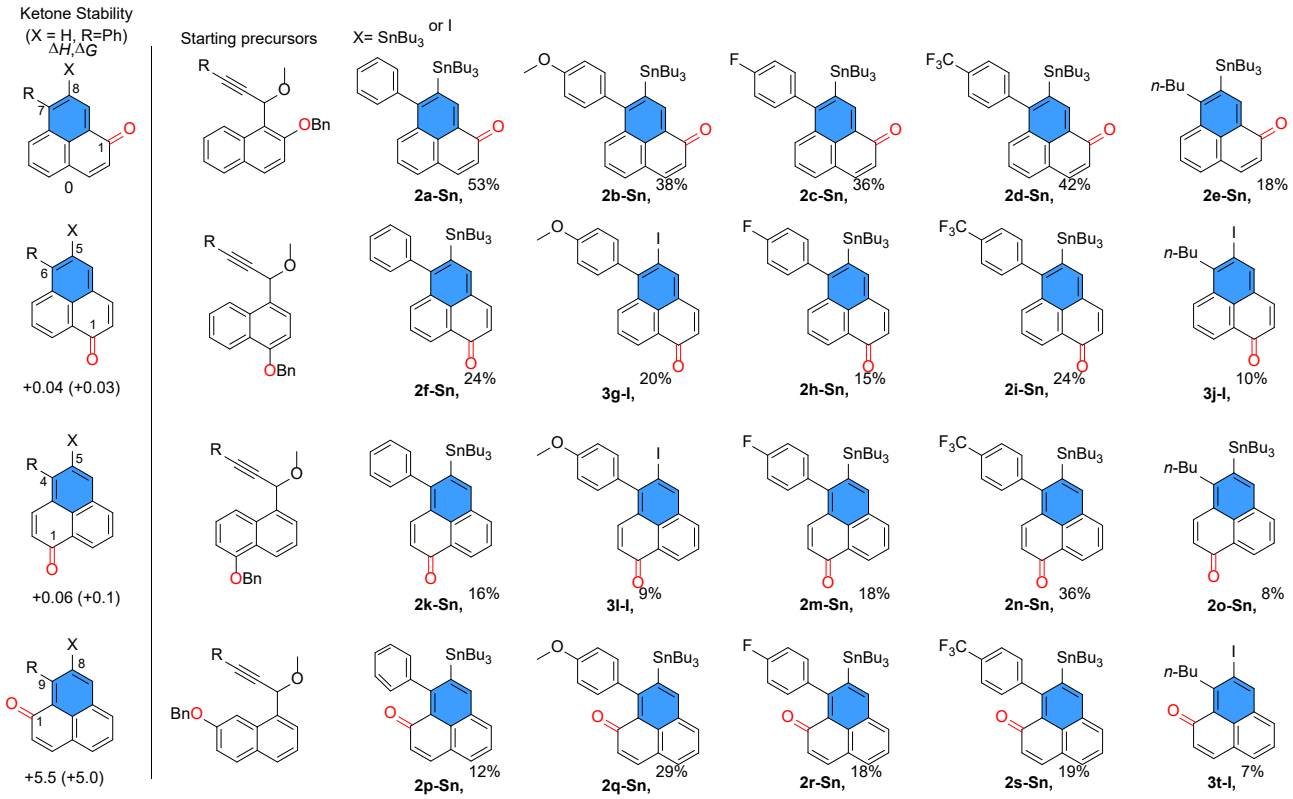

Figure 5. Scope of substrates for radical cyclization and the relative stability of ketones.

Synthesis of π-extended phenalenones

Encouraged by the success of the *peri*-cyclization/fragmentation sequence, we have explored the possibility of incorporating such sequence in an even longer cascade that are initiated by exo-dig cyclization of bis-alkynes. We have shown earlier that exo-dig cyclizations are stereoelectronically preferred over endo-dig cyclizations[134] for the conversion of skipped oligoalkynes into carbon-rich polycyclic structures via radical chemistry.

An interesting feature of such cascades is that, depending on the choice for termination step, they can open access to various extended polycyclic systems. If the radical cascade is propagated by exo-dig cyclizations, the last of such cyclizations gives a highly reactive vinyl radical. The latter is capable of addition to the terminal phenyl ring to give a five-membered ring cycle (Scheme 3a). Such five-membered rings can be used as a sites for additional transformations.[135–138] If presence of a five-membered ring in the product is undesired, it can be avoided by introduction of an alkene in the reaction cascade. In such a scenario, a 5-exo-trig cyclization at the final stage generates a less reactive alkyl radical, which is unable to attack the aromatic ring. Since the last cyclization step is blocked, a "defect"-free hexagonal polyaromatic framework is formed (Scheme 3b).[139]

Here, we synthesized π-extended phenalenones by exo-dig cyclization of bis-alkynes involving *peri*-cyclization/fragmentation sequence. This is a new strategy for termination of exo-dig cascades of substrates with multiple alkyne units. When the vinyl radical formed at the end of the alkyne cyclizations attacks the naphthalene *peri*-position, a 6-membered ring is formed. Importantly, the new polycyclic product has not five-membered "defects" and hence can be considered as a graphene substructure. However, this particular ring system is very different from a typical polyaromatic system because it has an odd number of carbons. Hence, it can be considered as a "π-extended phenalenyl". Because such species has multiple reactive sites based on the delocalized spin density, its subsequent reduction or oxidation reactions can potentially lead to multiple products e.g., isomeric phenalenes (after reduction) and ketones (after oxidation). Not surprisingly, our attempts to harness *peri*-cyclizations as the last step of such alkyne cascades fully illustrate this complexity, providing inseparable mixtures of many products. To address the problem of selectivity, an -OR group can be attached at four different positions of the "π-extended phenalenyl" to selectively direct the ketone formation (Scheme 3c).

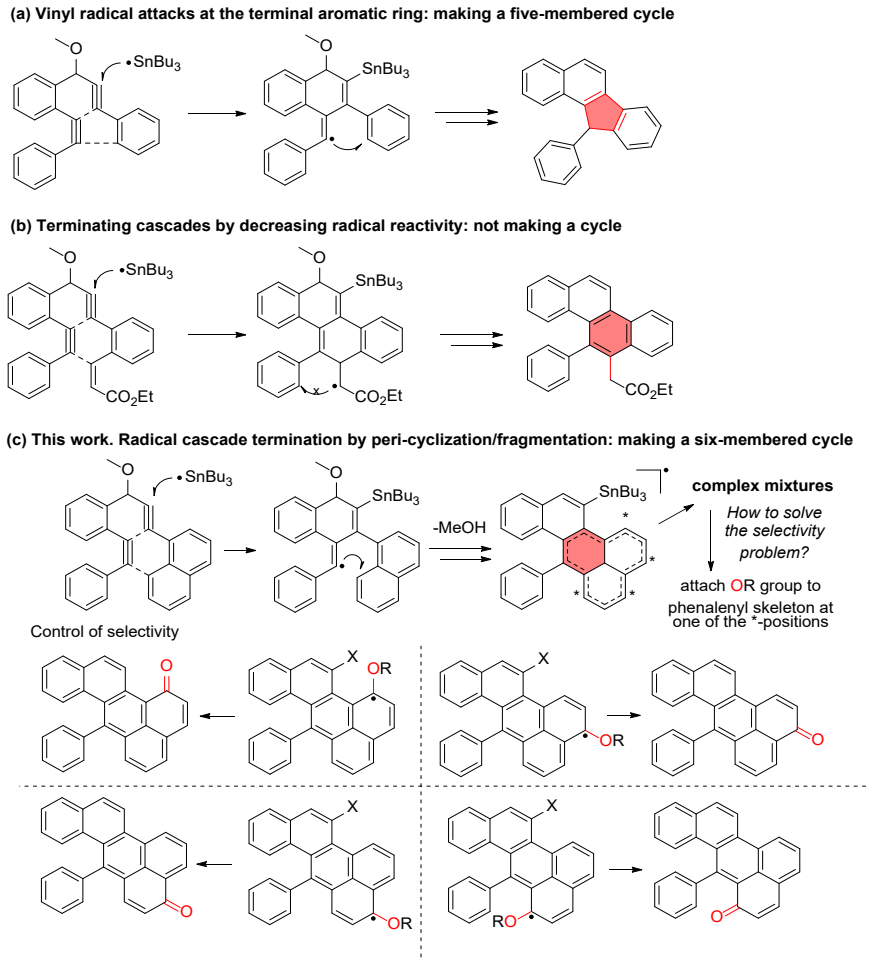

Scheme 3. Strategies for termination of exo-dig cascades. (a) Vinyl radical attacks at the terminal aromatic ring. (b) Terminating cascades by decreasing radical reactivity. (c) *Peri*-attack follows radical cascade termination by fragmentation. Note that (b) and (c) avoid incorporation of a five-membered ring in hexagonal framework.

The four bis-alkyne precursors were prepared from the nucleophilic addition of different lithium acetylides to the same aldehyde (Figure 6a). Three of these precursors reacted to form selectively one of the four isomeric expected π-extended phenalenones (**4a-H**, **4b-H**, **4c-H**). Only one of the four substrates did not form the cyclized product, most likely due to unfavorable steric factors. The structures of the three pentacyclic ketones were unambiguously confirmed by X-ray analysis (Figure 6b).

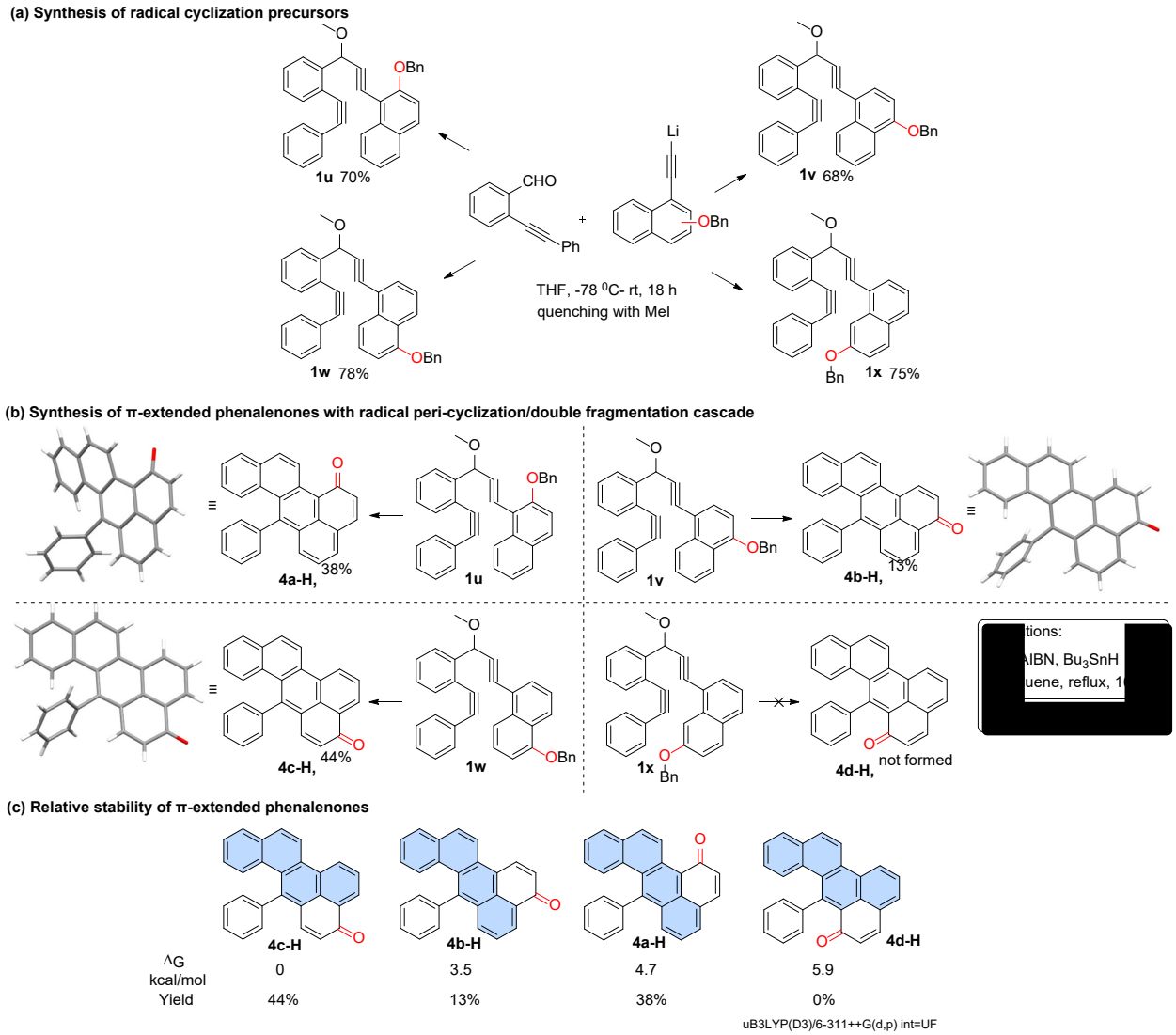

Figure 6. (a) Synthesis of π-extended phenalenones. (b) The relative stability of π-extended phenalenones. (c) Relative stability of π-extended phenalenones.

Computations were performed to gauge the stability of the four ketone isomers (Figure 6c). The most stable ketone gave the highest yield while the least stable one (5.3 kcal/mol higher in energy than the most stable ketone) was not formed. However, computations do not align with the experimental yields of the ketones **4a-H** and **4b-H** with the intermediate stability. The computationally less stable ketone (4.7 kcal/mol relative to most stable ketone) provided 38% yield while the slightly more stable ketone (3.5 kcal/mol) gave only 13% yield. A possible explanation is that the OBn group in precursor **1u** has an additional role. Not only does it direct the selective formation of the ketone, but it acts as a blocking group that prevents the competing five-membered ring formation. Comparison with the failed cyclization of **1x** illustrates that steric effects can be either beneficial or detrimental depending on the circumstances.

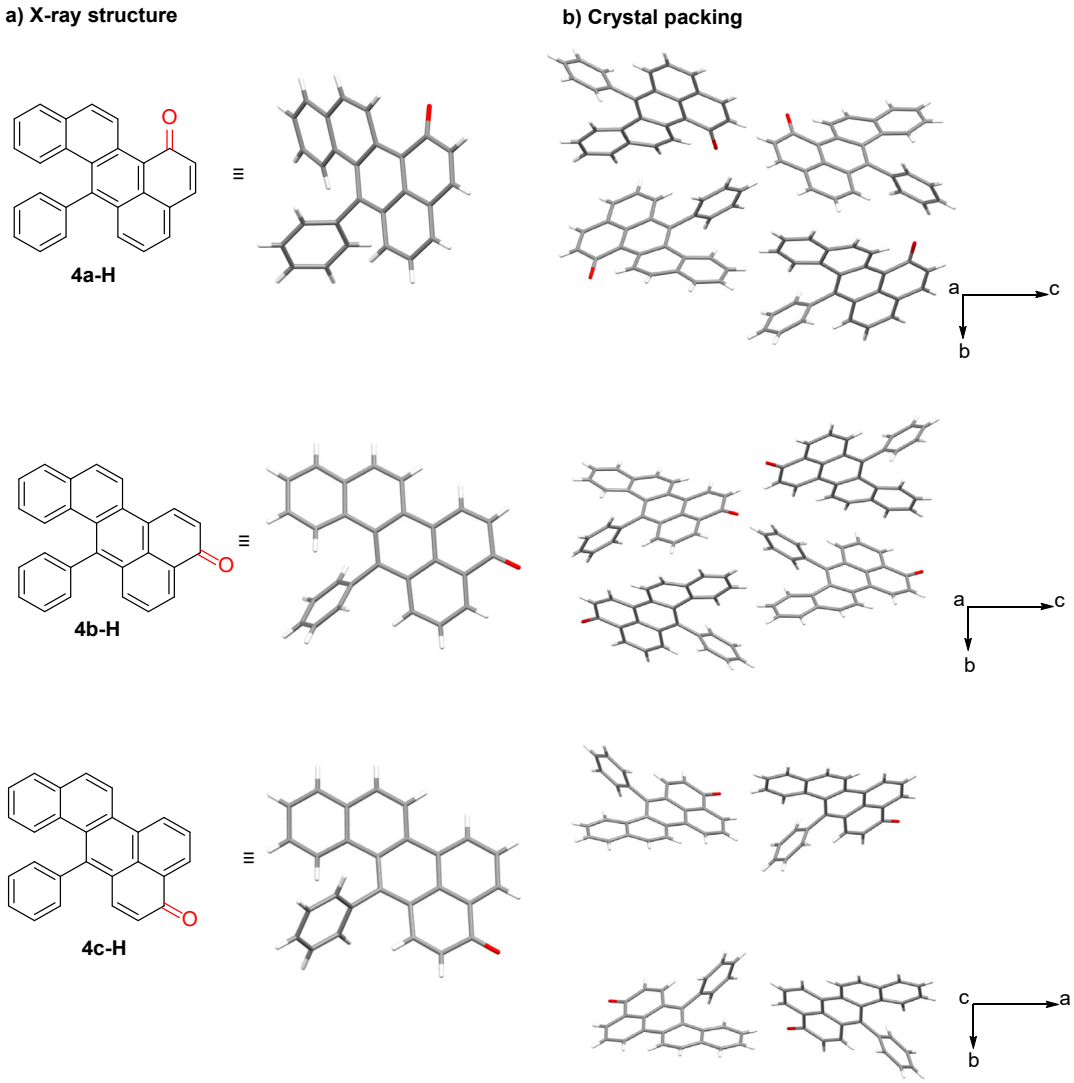

Figure 7. The X-ray structures (a) and crystal packing (b) for π-extended phenalenones.

Comparison of the X-ray geometries for the isomeric ketones revealed that the less stable isomer **4a-H** is more twisted because of a steric clash between the carbonyl oxygen atom and an adjacent C-H bond while the more stable ketones **4c-H** and **4b-H** are more planar (Figure 7a and 7b).

Polyaromatic Diones.

Polyaromatic diones are great potential candidates for precursors of organic open-shell species (Figure 1). However, the synthesis of polyaromatic diones often suffers from a lack of flexibility or a long sequence of steps. Our strategy shows great potential for systematically making a large library of polyaromatic diones by choosing different "links" between isomeric functionalized phenylphenalenones. Functionalized isomeric phenylphenalenones selectively synthesized by our strategy can be converted into different kinds of diones by subsequent cross-coupling reactions. The iodo-substituted phenylphenalenone was prepared easily from stannated phenylphenalenones. The structure was confirmed by X-ray crystallography. We used **3a-I** as an example to illustrate the feasibility of dione synthesis. The Sonogashira reaction of **3a-I** followed by deprotection gave the terminal alkyne **5**. Two

polyaromatic diones were made from alkyne **5**. The Glaser coupling of **5** gave dione **6** where two phenalenone units are connected by two alkynes. The Sonogashira coupling between **3a-I** and **5** gave dione **7** where two phenalenone units are connected by one alkyne (Scheme 4).

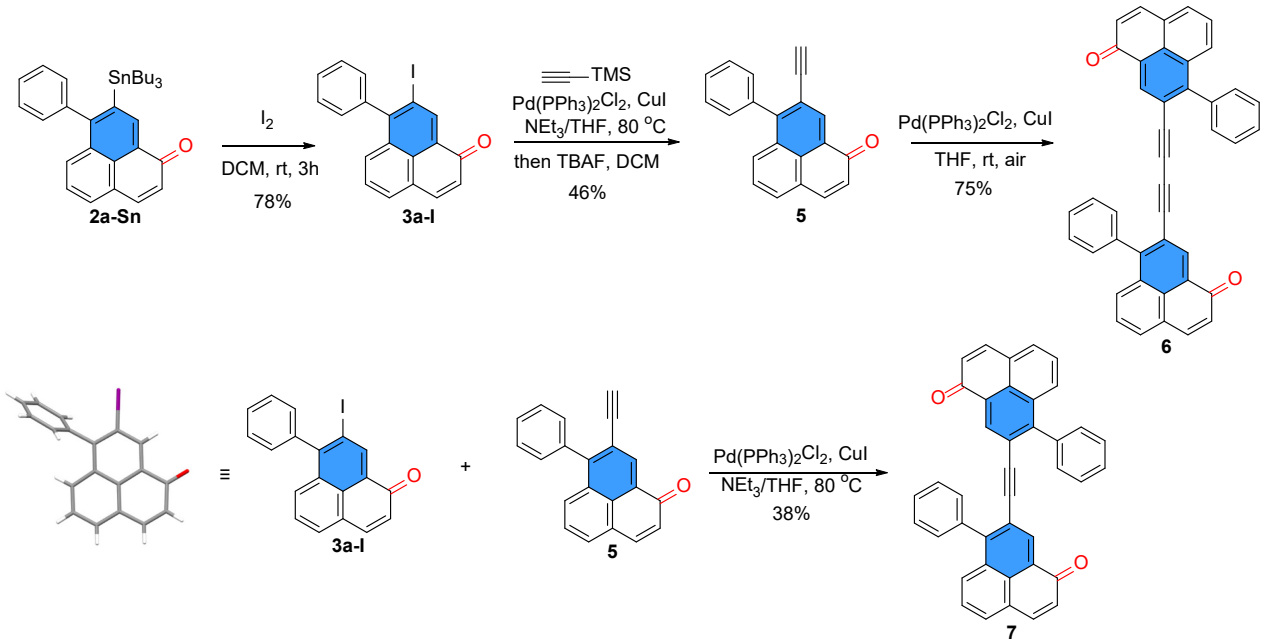

Scheme 4. Synthesis of polyaromatic diones from functionalized phenylphenalenones.

Computational analysis of possible cascade energy profiles

Multiple mechanistic possibilities for phenylphenalenone formation were explored computationally. All our proposed mechanisms start with $SnBu_3$ (approximated computationally as $SnMe_3$) radical addition to the alkyne, followed by the *peri*-annulation step, giving intermediate **A**. After this stage**,** one can envision numerous potential pathways towards the final product **2a-Sn**. The simplest scenario is shown in Figure 8. Guided by the Ockham's razor, we first considered the pathways where radical fragmentation proceeds directly from intermediate **A**. In Path 1, **A** loses methanol first to generate the naphthalene moiety in radical intermediate **B**. The subsequent C-O fragmentation will generate the final phenylphenalenone, **2a-Sn**. The alternative, Path B, starts with C-O bond fragmentation to generate a closed shell intermediate **D**. Aromatization of this intermediate via the loss of methanol provides the final product **2a-Sn**.

Interestingly, the transition state (TS) barrier for the first steps of Path 1 and Path 2 are similar (32.3 vs 32.7 kcal/mol, respectively). However, this step is highly exergonic in Path 1 (-43.0 kcal/mol), where aromaticity is restored, but endergonic (22.6 kcal/mol) in Path 2. Due to the endergonicity of the latter step, we expect it to be reversible (with a reverse barrier of only 10.1 kcal/mol) and Path 1 to be more important than Path 2.

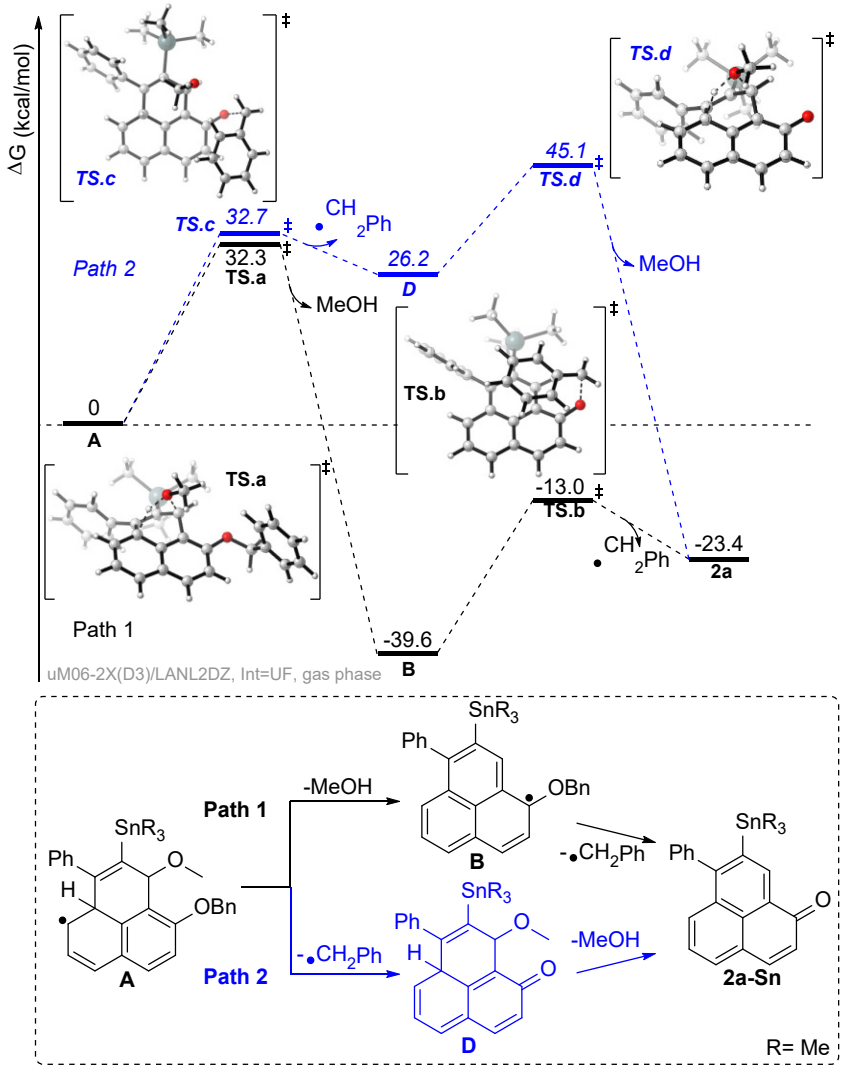

Figure 8. Initial mechanistic hypothesis for the two routes to phenylphenalenones formation. Note that a single radical center cannot efficiently promote both fragmentations.

Indirect mechanisms. One radical is not enough: radical cascade with multiple reentries.

Both Path 1 and Path 2 have rather large activation barriers. Although the barriers are traversable at the reaction conditions (110 °C), we elected to computationally explore if more favorable alternative pathways exist. Generally, one would expect C-centered radicals to find lower barrier reaction channels, especially in the presence of multiple functional groups.

Computational data suggests that there are two difficult post-cyclization steps: 1) aromatization of the top ring through loss of MeOH and 2) formation of the carbonyl via C-O scission resulting in the loss of the CH_2Ph radical. The concerted loss of MeOH is difficult because the large O….H distance leads to a highly strained TS geometry (**TS.a**, **TS.d**, Figure 8). Therefore, we searched for a lower barrier alternative pathway and found that the loss of the OMe radical is facile if the step is coupled with aromatization (an activation barrier of 14 kcal/mol (**TS.c**, **TS.h**, Figure 9) compared to the >20 kcal/mol barrier for the loss of MeOH, (**TS.a**, **TS.d**, Figure 8). However, for the loss of the •OMe group to be coupled with aromatization, the radical center must be 'para' to the departing •OMe moiety. As the initial *peri*-cyclization

(intermediate **A**) creates the radical at the 'wrong' "meta"carbon (Scheme 5), the radical needs to be translocated via a formal 1,2-shift in order for loss of the •OMe moiety to be coupled with aromatization.

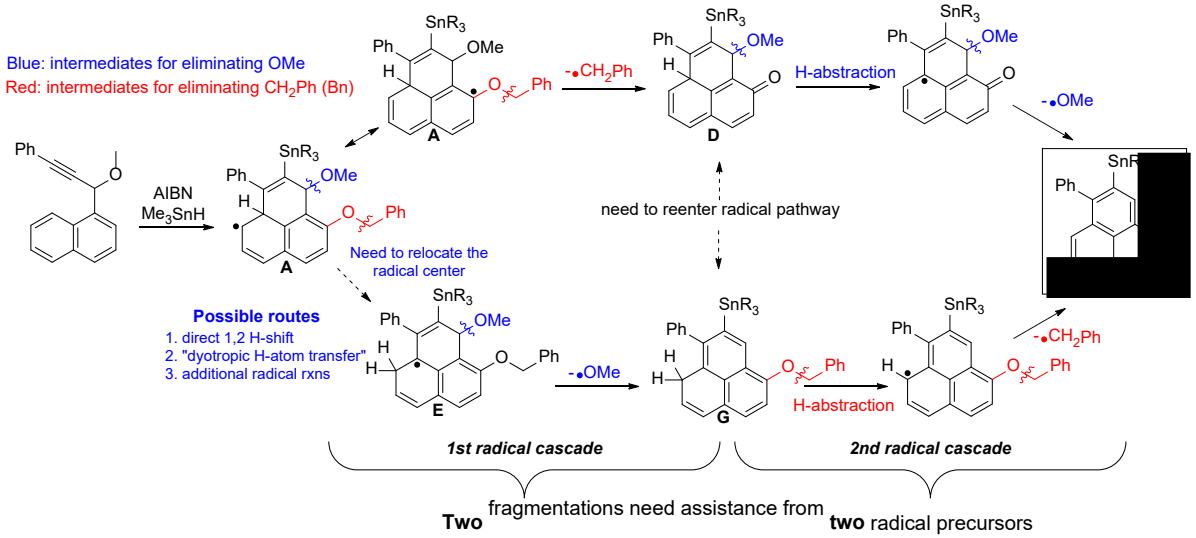

Scheme 5. The revised mechanistic scenario requires two radical fragmentations for the formation of the phenylphenalenone product, **2a-Sn**.

Considering the above, we explored multiple pathways that result in the required formal 1,2-shift. The most obvious solution would be a direct H-shift from **A** to give either **F** or **F'**. Unfortunately, both steps have an activation barrier of >30 kcal/mol (Figure S17). However, several indirect but potentially efficient paths to the final product can be uncovered if one takes into account the reversibility of radical processes, especially under reaction conditions where an excess of external radical species is introduced.[140–142] When radicals are abundant, they can engage in both bond making and breaking. Since radicals are chemical chameleons (an orbital with a single electron is both "half-full" and "half-empty"), they can interact with each other in a variety of ways. As a result, the key tricyclic radical intermediate **A** (i.e., the direct product of *peri*-cyclization) can be either reduced, or oxidized, or simultaneously reduced *and* oxidized via atom transfer reactions. We consider each of these three scenarios in the three following sections. Remarkably, each of these paths can be productive and, furthermore, the radical intermediates can cross between these paths.

Reductive termination of *peri*-cyclization and radical re-entry: A potential pathway involves a sequence of H-abstractions that effectively translocate a hydrogen using a •$SnMe_3$ radical (Figure 9). Both a 2,3- or 2,5-H shift will result in radical density delocalized onto the target 'para' carbon. In this pathway, the first radical hydrogen addition occurs from a $HSnMe_3$ moiety at the 3- or 5- position resulting in intermediate **E** and **E'**. Then, a •$SnMe_3$ radical can abstract the hydrogen in the 2-position finishing the sequence that leads to the desired formal 1,2-shift (intermediates **F** and **F'**). From **F** or **F'**, the loss of the •OMe moiety restores aromaticity in the top ring (activation barriers of 6.6 and 10.2 kcal/mol, respectively). As the radical departs, the reacting system is at a stationary closed-shell point and requires another activation step to reenter the radical path. This can be done by using the weakness of the doubly allylic C-H bonds present in both **G** and **G'**. Each of these allylic hydrogens can be abstracted by a •$SnMe_3$ radical converging on the penultimate radical intermediate, the phenalenyl **B**. The CH_2Ph radical extrusion from this intermediate results in the final product **2a-Sn**. Although these steps involve multiple radical intermediates, some of which may be short-lived, this scenario is consistent with the need for an excess

of R_3SnH and AIBN to obtain the highest reaction yields. The kinetics for this energy profile is more favorable in comparison to the direct "one-radical / two eliminations" path presented earlier in Figure 8. Although the final fragmentation is endergonic, the overall process can be made thermodynamically favorable once the departing benzyl radical is trapped in a subsequent exergonic reaction.

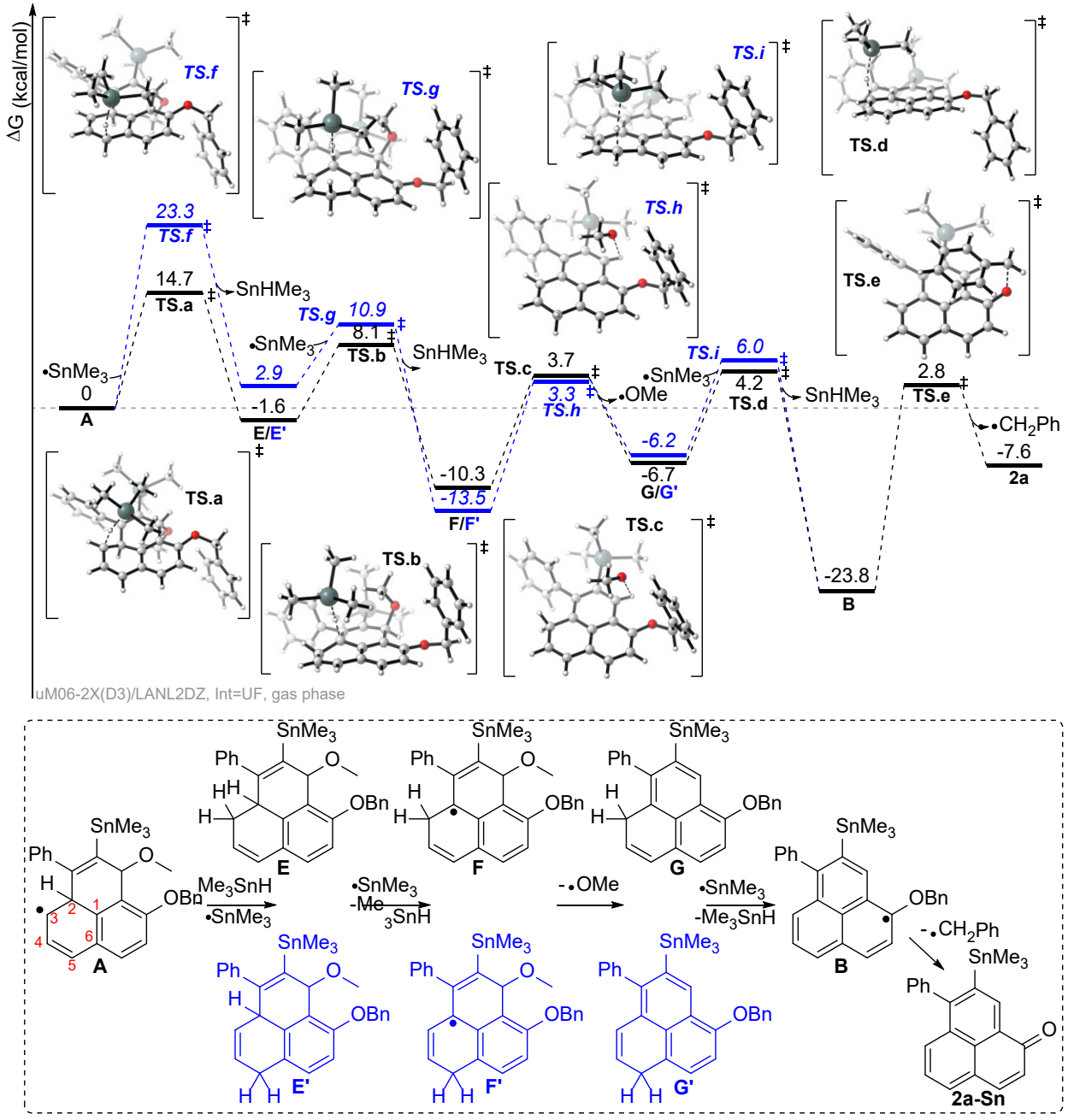

Figure 9. The indirect path to the formal 1,2-hydrogen shift is needed to form a radical center that can assist the fragmentation reactions. Reductive termination with re-entry.

Oxidative termination of *peri*-cyclization and radical re-entry: Another possible path to the product involves an exit from the radical path via H-atom transfer (HAT) *from* intermediate **A** to the AIBN-derived radical (or another species from the radical cocktail present in the reaction mixture). This is a formal oxidation (H-atom is removed from **A**). This direction deserves to be considered because HAT leading to the aromatized intermediate product **E''** is very exergonic (-66.1 kcal/mol, Figure 10). Alternatively, AIBN is known to act as an H atom trap, so it can transform intermediate **A** to **E''** with the formation of reduced diamine.[143] The intermediate product **E''** can be transformed into the observed final product **2a-Sn** via a sequence of steps that can be considered a "radical catalysis" by Sn-radicals.

In the first step, the closed-shell product **E''** is converted back into a radical through the addition of •$SnMe_3$. There are multiple positions for this radical's attack at the conjugated π-system of **A** that will provide the addition product with spin density at the β-carbon next to the OMe group. Figure 10 shows only one of such possible intermediates, i.e., the conjugated radical **H** formed via the intermolecular attack at a sterically unhindered position. The loss of •OMe from this intermediate is facile because it is assisted by aromatization in the top ring. Again, the system leaves the radical cascade and forms a closed shell intermediate, **I**. Remarkably, the Sn-C bond formed in the previous step is relatively weak and can be broken (either homolytically or via an intermolecular reaction with either the •OMe or an AIBN-derived radical) with the formation of intermediate **B** in a barrierless reaction (Figure S20). This radical has spin density at a position that is suitable for assisting in the loss of the •CH_2Ph moiety that generates the final product **2a-Sn** in Figure 10. Conceptually, this is an intriguing and elegant sequence as *such assistance of a R_3Sn-radical would be catalytic and traceless*. The R_3Sn adds and then departs, changing functionality in its tricyclic "substrate" between the two steps. The initial R_3Sn introduction generates a radical at one position where it leads to a productive transformation (elimination of •OMe). The subsequent R_3Sn departure generates a radical at a different position where productive C-O bond fragmentation can occur. Remarkably, neither of the two radicals are wasted – both assist in a radical fragmentation.

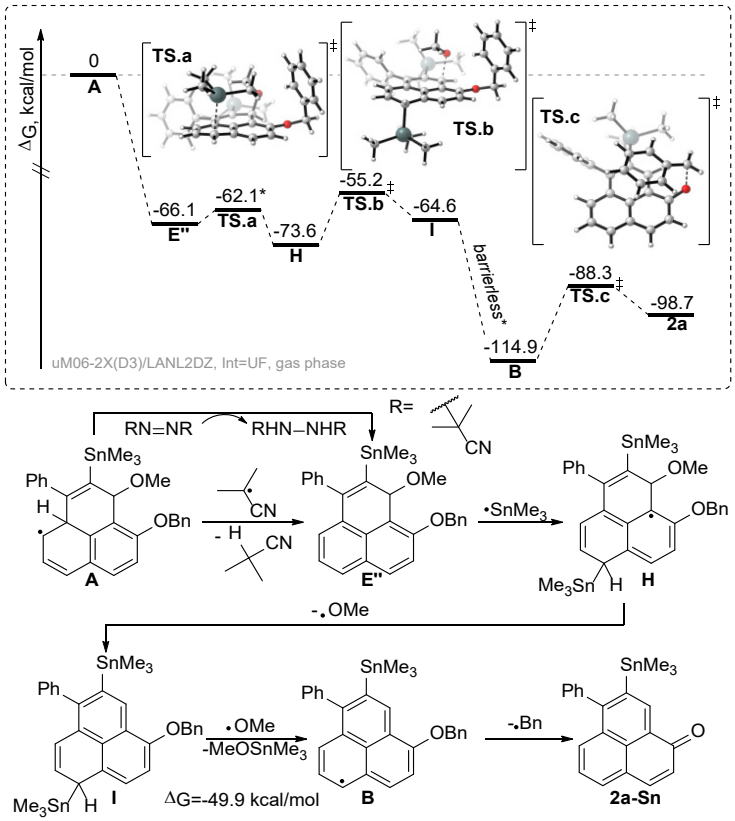

Figure 10. "Radical catalysis". An alternative path to the final product: temporary exit of the radical cascade by formal oxidation with subsequent reentries by addition and elimination of a R_3Sn radical. The Sn-radical addition step generates a radical that can assist in the •OMe departure while subsequent scission of the same C-Sn bond that was formed in the addition step generates a different radical that can assist in the $PhCH_2$-O scission. * See SI for details of TS search.

Disproportion with an external radical – a formal intermolecular dyotropic rearrangement with a trifurcation: The final potential pathway to achieve the formal 1,2-shift is a disproportionation path (Figure 11). We will show below that it can lead to formal oxidation or reduction (both with a temporary loss of the radical character) or exchange H-atoms without loss of radical character. The latter path is neither oxidation or reduction since one C-H bond is broken while the other C-H bond is formed simultaneously.

An intriguing feature of the latter path is that it has resemblance to a dyotropic reaction. By definition, a dyotropic rearrangement involves two σ-bonds migrating simultaneously (Figure 11a).[144–149] Generally, dyotropic reactions are concerted and, to the best of our knowledge, all of the reported literature examples are intramolecular. The present case is different as it involves an *inter*molecular transfer of two groups between *two* molecules. Equally intriguing is that the participating partners are two open-shell species. However, despite these unusual features, the transformation does formally fit the definition of a dyotropic process. Furthermore, the similarity to classic pericyclic reactions is emphasized by the potentially aromatic six-electron cyclic transition state (shown in Figure 11b for the interaction of two ethyl radicals).

For simplicity, let us consider first the intermolecular 'dyotropic-like' H-atom exchange between two ethyl radicals in Figure 11b.[150,151] The transition state for the 'dyotropic' pathway is downhill by 3

kcal/mol! This is possible because the high energy ethyl radical state crosses with the low energy neutral ethane + ethene potential energy surface at the transition state. In other words, the symmetric TS for the two H-atom transfers between the two radicals is indistinguishable for the TS for H_2 molecule transfer between ethene and ethane. Therefore, the two ethyl radicals go through a negative activation barrier before continuing to the lower energy ethane + ethene state.

A similar pathway is possible in our system. We start with two high energy radicals, **A** and an AIBN-derived radical. The activation barrier for the formal 1,2-shift is 5.6 kcal/mol, however, this TS crosses with the energy surface of the disproportionation pathway (which has a barrier of 39.4 kcal/mol for the same TS) (Figure 11c). At this cross-over point there are three potential outcomes: 1) the desired 1,2-shift product (**F** and a different AIBN-derived radical), 2) disproportionation resulting in **E''** and a quenched AIBN radical, or 3) returning to the reactant of the crossed energy surface (**E** and methacrylonitrile). Unfortunately, the desired 1,2-shift product is a high energy state (>30 kcal/mol higher in energy than the other potential products) and unlikely to be formed in comparison with the other two potential products (Figure 11d). However, this is likely to be of little consequence as the other two products correspond to the oxidized (**E''**) and reduced (**E**) descendants of the parent radical **A**. Both **E** and **E''**, can be converted into the final product as we have shown in the previous two sections.

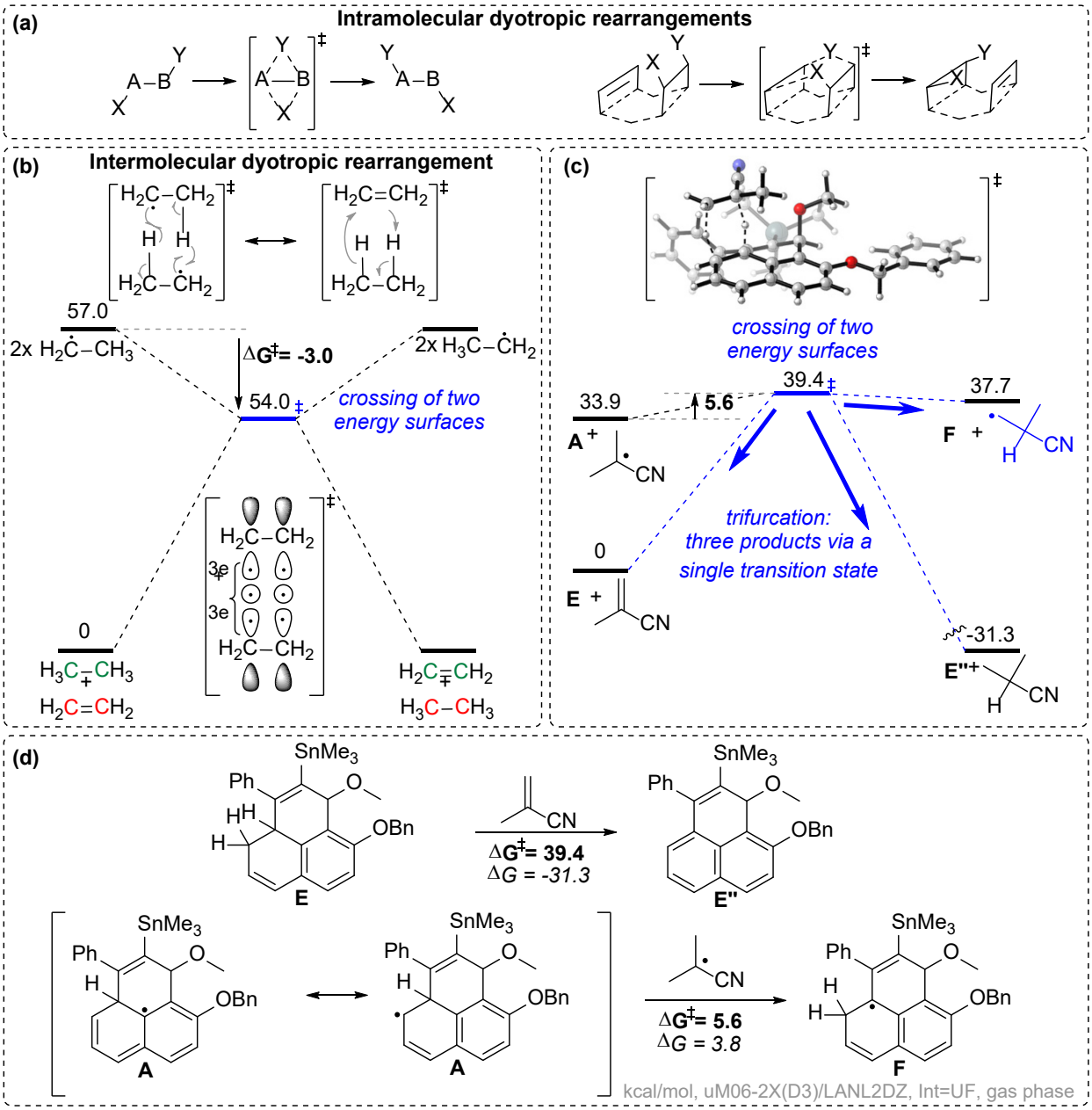

Figure 11. (a) Examples of the two types of intramolecular dyotropic rearrangements.[145] (b) The intermolecular dyotropic rearrangement and its relation to disproportionation for the case of two ethyl radicals. (c) A potential dyotropic rearrangement from the high energy radical state of intermediate **A**. (d) The two reaction pathways depicted in part c.

Experimental detection of multiple radical species at the different stages of the cascade

In order to get insights into the mechanistic complexity suggested by the computational analysis, we have conducted spin trapping experiments with the aim of capturing radical species that are present at different reaction times. Four separate reactions were carried out, each different from others only by the time of addition of the spin trap. We have used two equivalents of 5,5-dimethyl-1-pyrroline N-oxide (DMPO), a versatile spin trap which has been used to trap oxygen-, nitrogen-, sulfur- and carbon-centered radicals.[152–155]

Spin-trapped products in the reaction mixtures were detected by mass spectrometry and summarized in Table 2 below (see SI for the additional information). Several conclusions can be made. First, the presence of multiple DMPO adducts confirms that the cascade is a multistage radical process where several types of radicals are involved. Furthermore, the evolution of trapped products illustrates the evolution of radical species that are born, transformed, and perished at the different stages of this multistage process.

Table 2. Detection of spin-trapped species by mass spectrometry illustrates formation and evolution of multiple radical species throughout the radical cascade.

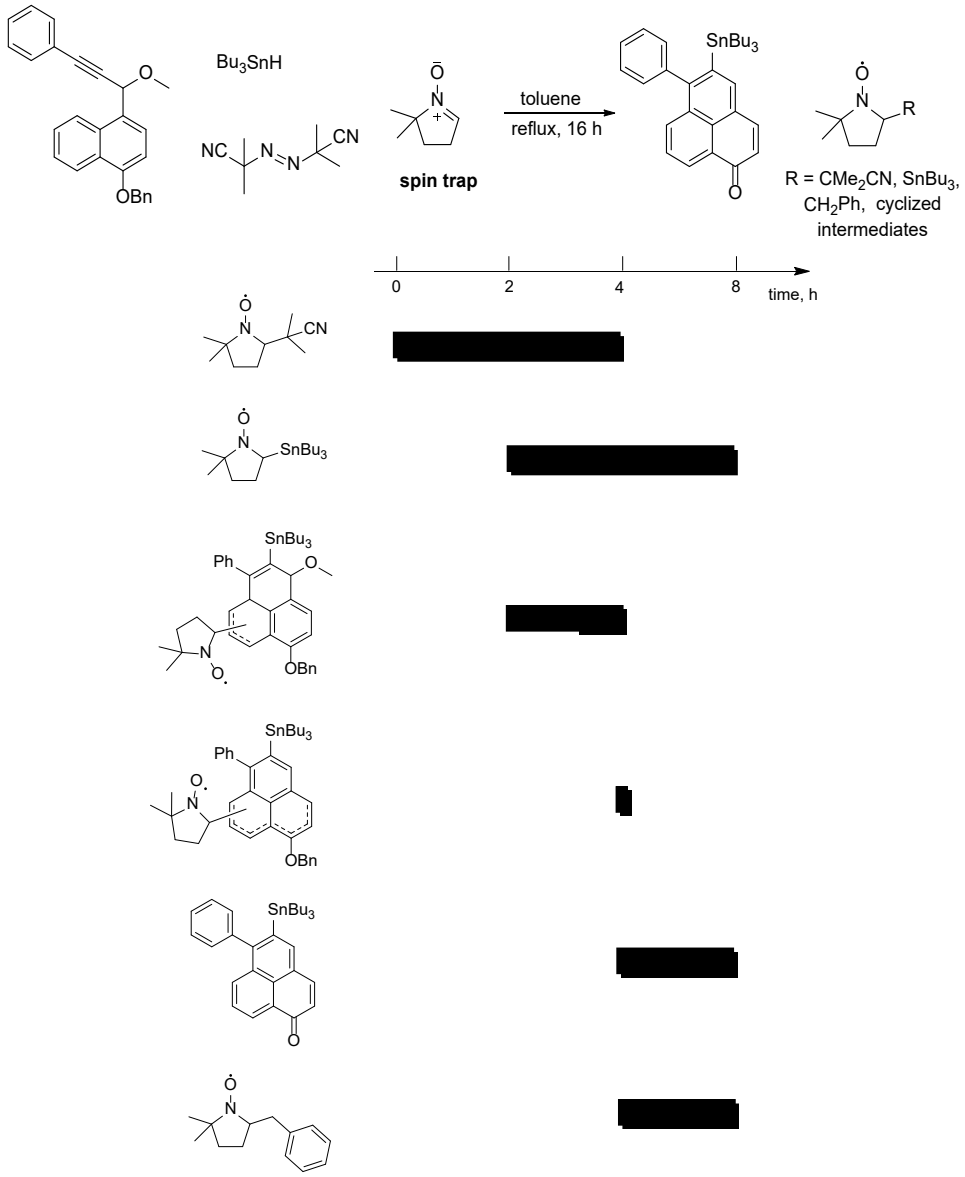

It is interesting to analyze how the nature of the transient radical species changes as the reaction proceeds. When added at the beginning, DMPO traps only $(Me)_2CCN$ (the radical generated via AIBN fragmentation), confirming that AIBN is indeed the first source of radicals, i.e., the cascade initiator. Addition of the spin trap after 2 h traps the AIBN-derived radical, the Bu_3Sn radical and the first cyclized

radical intermediate which still bears the MeO and $PhCH_2$ moieties, i.e., both of the potential leaving groups. Note the absence of the phenalenone product at this stage (fully consistent with the NMR results presented in the SI, Figure S1). The continuous presence of Sn-centered radicals throughout all reaction stages agrees with the "reductive termination with reentry" pathway, which depends on the reversible formation of such radicals at the intermediate stages of this reaction, as shown in Figure 9.

After 4h, the spin trap reports the appearance of $PhCH_2$-radical and the last radical intermediate that leads to product formation. Importantly, only at this point, we also see the beginning of the product formation. This result suggests that the final product originates from a $PhCH_2$- radical fragmentation, providing support to our hypothesis of the final step (carbonyl formation) mediated by the O-CH_2Ph bond scission. Clearly, the capture of this cyclized radical intermediate bearing only $PhCH_2$ moiety provides strong experimental evidence that the departure of the MeO group precedes that of the $PhCH_2$ group.

After 8 h, radicals derived from AIBN are not detected but $SnBu_3$ radical is still present, an evidence for $SnBu_3$ radical re-entry in the proposed mechanism. The fact that $SnBu_3$ radical is the only initial radical that remains half-way through the reaction time again suggests the cascade's preference for the reductive termination pathway (Figure 9) over the oxidative route (Figure 10). This is consistent with the absence of $MeOSnBu_3$ as well as the doubly stannylated intermediate **I** proposed in the oxidative termination pathway (Figure 10).

Interestingly, we did not detect the DMPO-OMe adduct in any of the four experiments. This can be explained in two ways: either 1) the initial hypothesis was wrong and the MeO fragment does not depart as a radical, or 2) the OMe radical reacts faster with a different partner. For the first scenario, one can consider deprotonation of the radical[156] to form a transient radical anion that can lose the methoxide anion. Computational data disfavor the anionic path as the radical-anion fragmentation is predicted to be strongly endergonic (ΔG = 34.8 kcal/mol). Moreover, removal of a β-proton, the requisite preceding step for MeO anion departure, is even more uphill in the absence of a strong base. It is also possible that, due to the relatively high oxophilicity of tin, OMe radical reacts with intermediate compounds with weak C-Sn bonds (such as dearomatized intermediate **I** in Figure 10) faster than with the trap. Such reaction with the formation of intermediate **B** and $MeOSnMe_3$ is ~50 kcal/mol exergonic (see the SI).

It is noteworthy that only the relatively nucleophilic radical species, namely $SnBu_3$, $(Me)_2CCN$ and other C-centered radicals, were captured while MeO radical, an electrophilic species, was not.[157] While DMPO is suitable for trapping MeO radical,[152] the rate of this reaction is likely to be lower than the reaction of DMPO with nucleophilic radicals. Hence, if $SnBu_3$ and $(Me)_2CCN$ radicals are also present and more abundant, they may with react with DNPO instead of the relatively electrophilic MeO radical.

Analysis by EPR spectroscopy further confirmed the formation of different radicals at different stages of reaction (see the SI). Unlike the mass-spec, EPR does not provide the formulas for each of the radical species but it has clearly confirmed the fact that the nature of radical species changes as the reaction proceeds.

Role of thermodynamics in radical fragmentation steps

We explored the thermodynamics of C-O radical fragmentation in order to find methods to increase the favorability of the intended fragmentations. The formation of the carbonyl via C-O scission resulting in the loss of the CH_2Ph radical is unfavorable by 16 kcal/mol (Figure 8). Analysis of the fragmentation step summarized in Figure 12 illustrates the effect of aromatic stabilization and radical delocalization on the thermodynamics of this key step. Not surprisingly, in the first equation going from a non-radical to two radical intermediates by breaking the C(sp^3)-O bond in anisole and generating an O-

radical and a CH_3-radical is highly unfavorable (eq. 1, Figure 12). This fragmentation is nearly half as endothermic when one starts with a radical reactant (eq. 2). The C-O fragmentation can be made less unfavorable by coupling the fragmentation with a gain in aromaticity or conjugation in the non-radical product (eq. 3-5). Finally, the role of radical delocalization in stabilizing the product was explored. The thermodynamic cost of fragmentation can be lowered by stabilizing the departing radical as either a phenyl or diphenyl group (eq. 6 & 7).

These equations highlight three factors to be considered in the design of the radical C-O bond fragmentations for lowering their thermodynamic cost: 1) starting with an open-shell radical reactant, 2) pairing fragmentation with a gain in stabilization (through conjugation) in the closed-shell product, and 3) stabilization of the departing radical through delocalization of the radical. When all three of these factors are combined the thermodynamic penalty can be lowered to 8.0 kcal/mol (eq. 8) compared to the nearly 52 kcal/mol thermodynamic penalty in eq. 1. Unfortunately, the C-O scission where a carbon-centered radical is formed is still endergonic (eq. 5, 6, and 8). Although the penalty is not prohibitive, it may indicate that the fragmentation step needs to be assisted by a fast exergonic reaction, such as capture of the departing radical, as well as by the high reaction temperature.

The other necessary C-O fragmentation results in an oxygen-centered radical (instead of the previous carbon-centered radical). All three of these factors contribute to the exergonicity of eq. 3, where the loss of a delocalized OMe radical is coupled with the gain of aromaticity in the closed-shell product. Implementing our findings from these thermodynamic equations to our reaction results in only a small thermodynamic penalty, eq. 9 and 10.

Role of thermodynamics of radical C-O bond fragmentation in different systems

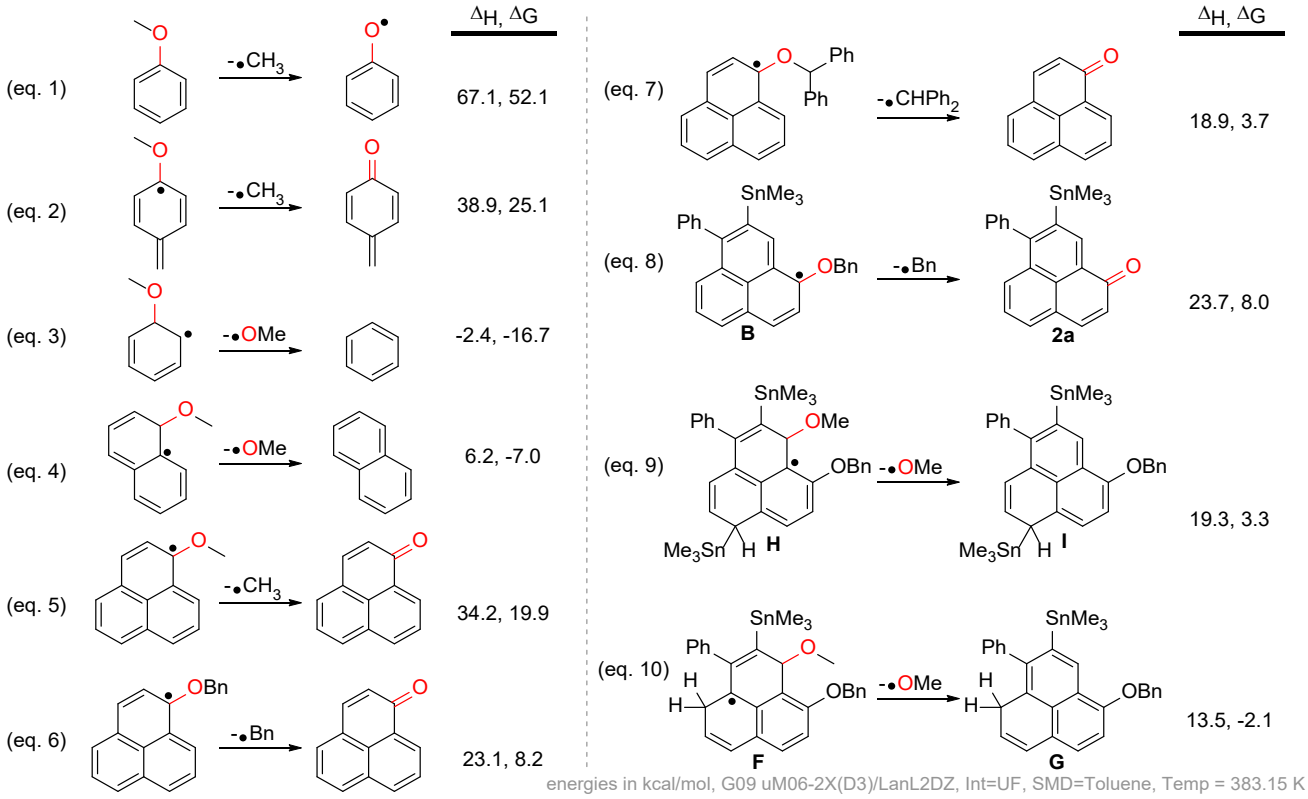

Figure 12. Role of thermodynamics of radical C-O bond fragmentation in different conjugated systems. Note that carbonyl-forming fragmentations are more favorable than benzylic C-O scission, even though the latter leads to a highly stabilized phenoxy radical.

Photophysical Properties

Phenalenones and their derivatives have rich photophysical properties[158,159] and they are known as good singlet oxygen photosensitizers.[160–165] Substituents on phenalenones and structural variations can strongly influence the photosensitizing properties.[166,167] Inspired by our library of structurally diverse functionalized phenalenones, we explored the relationships between their structure and properties. To compare the photophysical properties for the isomeric conjugated ketones, we analyzed absorbance and emission spectra for selected compounds (Figure 13).

In this family of isomeric phenylphenalenones (Figure 13a), compounds **2p-Sn** and **2k-Sn** show noticeable differences absorption spectral profile relative to **2a-Sn** and **2f-Sn**. Absorption of **2k-Sn** has a ~10 nm red shift relative to **2p-Sn**. This feature can be attributed to the positions of the three substituents (the ketone, the alkene, and the Ph group) relative to the common naphthalene core of the four isomeric compounds. On the other hand, change from an aryl to an alkyl substituent in the two ketones with the same core (**2a-Sn** and **2e-Sn**, Figure 13b) leads to nearly identical absorption spectra, indicating that the nature of this substituent does not have a large effect on electronic structure of the chromophore. This is consistent with the observations from the X-ray geometries that clearly indicate that the pendant aromatic substituents are nearly orthogonal to the tricyclic chromophore core.

For the family of π-extended phenalenones (Figure 13c), the absorption spectra of all three isomers are red-shifted in comparison to the spectra of parent phenalenones **2**. However, the position of absorption peaks changes considerably depending on the structure. The absorption of ketone **4c-H** is blue-shifted relative to the absorption of ketone **4a-H** and **4c-H** (by 40 and 80 nm, respectively). These large differences stem from the variation in the electronic nature of the tetracyclic aromatic cores of the respective chromophores, i.e., the chrysene unit in ketone **4c-H** vs. the benz[a]-anthracene units in ketone **4a-H** and **4b-H**. Chrysene has a higher HOMO-LUMO gap than benz[a]-anthracene (tetraphene).[168] Both of the diketones, **6** and **7**, have absorption maxima that are similar in energy to that of the individual ketone subunit, suggesting that electronic communication between the two phenalenyls in these two systems is relatively small.

Emission from a cross section of the compounds were measured and the results are summarized with Table S2. The emission energy generally tracks with the trend in absorption with the π-extended phenalenones being the most red-shifted (>480 nm) and the pheylphenalenone and phenalenyl diketones exhibiting similar emission energies from 420-440 nm. Aside from **4a-H** (Φ_{FL} = 0.01) and **4b-H** (Φ_{FL} = 0.08), the emission quantum yield was <0.1%. Presumably the increased rigidity of the π-extended phenalenones derivatives decreases the non-radiative decay rates and increases the emission quantum yield. The lower emission quantum yield of **4c**, relative to **4a** and **4b** is consistent with the assigned fluorophoric core in Figure *6*c where chrysene emitters are typically less efficient than there benz[a]-anthracene counterparts.[169]

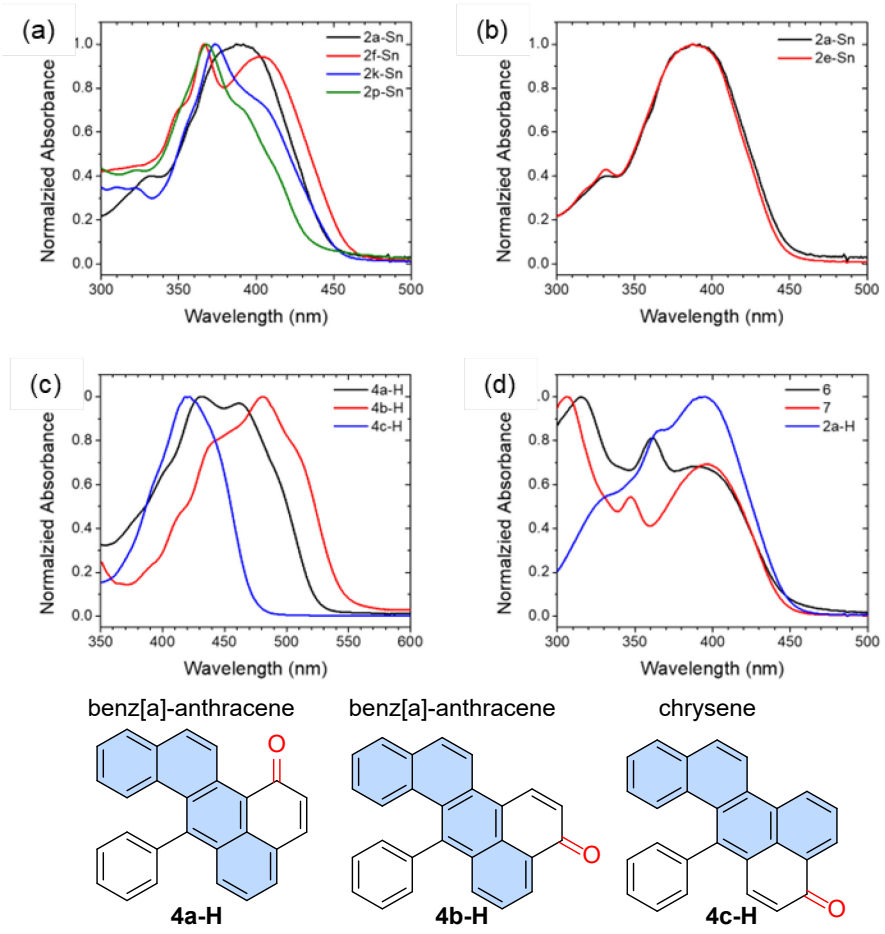

Figure 13. Normalized absorption spectra in dichloromethane for the (a) isomeric phenylphenalenones family; (b) phenalenones **2a-Sn** and **2e-Sn**; (c) isomeric π-extended phenalenones (d) alkyne-bridged phenalenyl diketones.

CONCLUSIONS

One does not need an oxidant to direct alkyne radical annulation cascades to the formation of formally oxidized products (e.g., phenalenyl ketones). The oxidized partially aromatized products can be selectively obtained without adding an oxidant via a controlled termination strategy. In this strategy, radical alkyne *peri*-annulations are extended to convert a pre-installed OR ether moiety into a keto group via radical O-R bond scission.

Attaching an O atom with a leaving group into the phenalenyl radical allows one to "capture" spin density at each of the resonance structures contributing to radical delocalization in the phenalenyl radical via a C-O bond fragmentation. The presence of the C-O bond "pre-programs" the substrate, so only one of the possible phenalenyl ketone products is formed selectively. An attractive feature of this approach is that the ketones are formed without the oxidation step that has been necessary for previous 1st-generation *peri*-cyclizations. Remarkably, even the least stable phenalenyl ketone isomers (up to 5 kcal/mol higher in energy than the most stable isomer) can be obtained from this newly designed double radical cascade. Although the yields are sometimes modest, the overall sequence includes four to five steps, so the 7-53% overall yields correspond to ~51-85% average yields for each of the individual steps.

Multiple potential pathways of the two radical cascades were explored computationally. From the post-cyclization radical intermediate **A** direct fragmentation of either of the two target C-O bonds is unlikely. Hence, the overall one-pot transformation requires two rounds of "post-cyclization" radical activation, referred here as the "radical cascade with a double re-entry".

Remarkably, each of the two additional stages in the extended sequence is terminated via C-O bond scission but leads to structurally different outcomes – a) loss of an alkoxy group with aromatization, and b) loss of an alkyl group with the carbonyl moiety formation. Both fragmentations are facilitated by the radical nature of the intermediates and, hence, once one cascade is terminated by the fragmentation that forms a non-radical intermediate, the 2nd sequence of radical transformations must be reinitiated, explaining the necessity of using one equivalent of AIBN (i.e., *two* equivalents of the AIBN-derived C-centered radicals). Interestingly, experiments with the DMPO spin trap clearly indicate that the radical species continue to be generated long after the AIBN-derived radical exit the stage. In particular, the Bu_3Sn radical is present throughout the whole process. The experimental evolution of partially aromatized C-centered radicals indicates that the loss of OMe group occurs first and the loss of benzyl radical happens at the final stage of the cascade. The order of steps in this sequence is fully consistent with the need to form an aromatic naphthyl moiety to compensate for the loss of aromaticity in a ring that is destined to become a cyclic enone after the O-Benzyl bond is cleaved (Scheme 6).

Although the product of initial cyclization has spin density at a position where it can potentially assist to O-Bn bond scission, the reaction is unfavorable because it would result in uncompensated loss of aromaticity at the O-Bn-substituted ring. Pre-aromatization of the adjacent OMe-substituted ring is needed to make that loss inconsequential. Computational evaluation of the possible scenarios suggests multiple pathways for the loss of OMe-group which are consistent with the combined experimental and computational data. These pathways include additional radical reactions needed to move radical centers at the positions where the radicals can assist in β-bond scissions. For example, an intriguing "radical catalysis" sequence, where a weak C-Sn bond is formed and broken reversibly, can inject an activating radical center at each of the two sets of positions within the tricyclic system (stars and circles in Scheme 6). The need for additional radical reactions agrees very well with the experimental necessity for the excess AIBN and Bu_3SnH.

The general importance of this work is that it reveals a working radical cascade outside of the usual paradigm of efficient radical chain reactions. Even when the chains are broken, the radical cascades can be restarted, first with the excess of radical initiator and then via reactivation of transiently formed weak covalent bonds. This design provides another connection between radical chemistry and dynamic covalent chemistry. [140] The presence of weak benzylic/allylic C-Sn bonds accounts for the generation of Sn-centered radicals throughout the multistage cascade sequence.

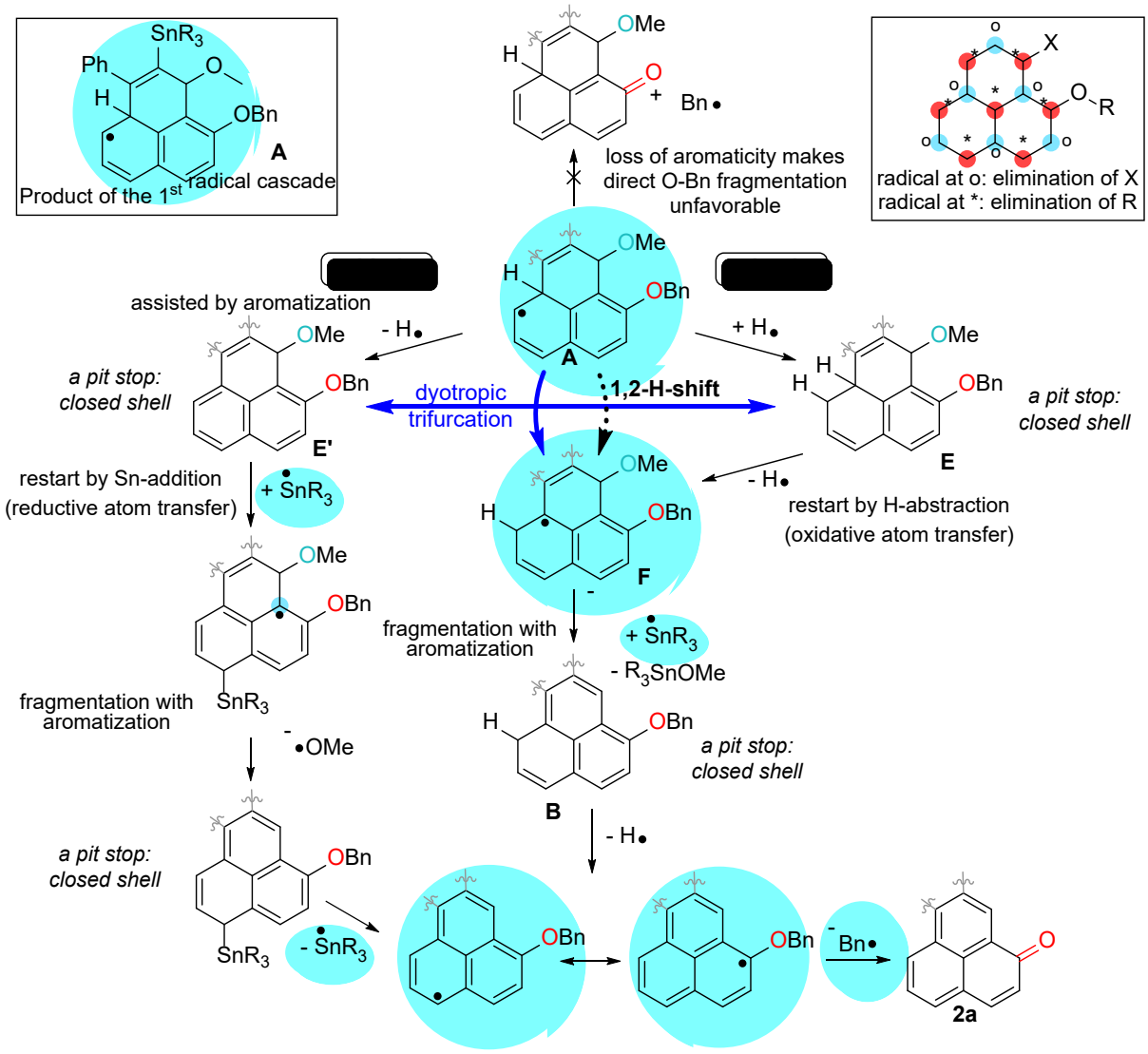

Scheme 6. A conceptual summary of the "multiple reentry" radical cascade that takes the initial peri-cyclization product through the sequence of two radical C-O fragmentations. Arrows are shown in the direction that indicates progress towards the final product. Under the reaction conditions, some of these reactions can be dynamic equilibria. Note that radicals must be formed transiently at any carbon in each of the two sets of phenalenyl carbons (labeled here as * and o). A radical at any carbon in one of these sets is suitable for assisting in one of the two C-O fragmentations. Radicals experimentally detected through spin-trapping experiments are placed in highlighted blue circles. Also note that the Bu_3Sn radical is present throughout the whole process.

We have further expanded this design for termination of radical *exo-dig* cyclization cascades of bis-alkynes in which *peri*-attack of the vinyl radical intermediate at naphthalene creates "π-extended" phenalenyl unit. The OBn group at different position directs the carbonyl formation, giving isomeric π-extended phenalenones selectively. This strategy also provides "defect"-free hexagonal polycyclic framework that contains an odd number of carbons and, hence, is suitable for the synthesis of stable aromatic radicals. The Sn- and I-substitution that arises naturally from this chemistry lends itself to the

subsequent incorporation of such units into larger spin systems. Our future work will concentrate on transforming the new family of phenalenones into structurally diverse aromatic radicals and diradicals.

COMPUTATIONAL DETAILS AND METHODS

All calculations were carried out using Gaussian09[170] at the uM06-2X/LanL2DZ level of theory with Grimme's dispersion[171] (emp=gd3) in the gas phase with an ultrafine integral (int=uf) at standard temperature (293.15 K) (unless stated otherwise in the figure). The unrestricted M06-2X[172,173] functional is known to provide a relatively accurate description of reaction and activation energies for a variety of chemical processes including radical reactions.[98,138,174] Potential conformers for the proposed intermediates were explored using Conformer-Rotamer Ensemble Sampling Tool (CREST).[175] Frequency calculations were performed in order to verify the structure as a stationary point or transition state. IRC calculations were conducted on all transition state molecules to ensure they exist on the correct potential energy surface. Spin density images were constructed using IQmol[176]and transition state images were constructed using CYLview.[177]

ASSOCIATE CONTENT

Supporting Information

Full experimental details, ^{1}H NMR, ^{13}C NMR, NMR spectra for all of the prepared compounds, X-ray crystallography data for selected products, and computational details for all calculated structures.

ACKNOWLEDGEMENTS

This work is sponsored by the National Science Foundation (CHE-2102579). The Rigaku Synergy-S single-crystal X-ray diffractometer which was acquired through the NSF MRI program (award CHE-1828362). L. K. acknowledges support by the National Science Foundation Graduate Research Fellowship under Grant No. 1449440. This project used resources at the National High Magnetic Field Laboratory supported by the National Science Foundation (DMR-2128556) and the State of Florida. The authors are also thankful to the FSU NMR facility (FSU075000NMR). We dedicate this work to Dennis Curran on the occasion of his 70th birthday and in appreciation of his many seminal contributions to the field of organic radical chemistry.

REFERENCES

(1) Kubo, T. Phenalenyl-Based Open-Shell Polycyclic Aromatic Hydrocarbons. *The Chemical Record* **2015**, *15* (1), 218–232. https://doi.org/10.1002/tcr.201402065.

(2) Kubo, T. Syntheses and Properties of Open-Shell π-Conjugated Molecules. *BCSJ* **2021**, *94* (9), 2235–2244. https://doi.org/10.1246/bcsj.20210224.

(3) Ahmed, J.; Mandal, S. K. Phenalenyl Radical: Smallest Polycyclic Odd Alternant Hydrocarbon Present in the Graphene Sheet. *Chem. Rev.* **2022**, *122* (13), 11369–11431. https://doi.org/10.1021/acs.chemrev.1c00963.

(4) Morita, Y.; Suzuki, S.; Sato, K.; Takui, T. Synthetic Organic Spin Chemistry for Structurally Well-Defined Open-Shell Graphene Fragments. *Nature Chem* **2011**, *3* (3), 197–204. https://doi.org/10.1038/nchem.985.

(5) Murata, I.; Nakazawa, T.; Okazaki, M. 2-Ethoxy-9,10,11,12-Tetrachloropentaphenafulvalene. *Tetrahedron Letters* **1969**, *10* (24), 1921–1924. https://doi.org/10.1016/S0040-4039(01)88047-3.

(6) Murata, I.; Nakazawa, T.; Tada, S. The Chemistry of Phenalenium System. VI. Some Derivatives of Pyranylidenephenalene. *Tetrahedron Letters* **1971**, *12* (50), 4799–4802. https://doi.org/10.1016/S0040-4039(01)97619-1.

(7) Nakasuji, Kazuhiro.; Yamaguchi, Masakazu.; Murata, Ichiro.; Nakanishi, Hiroshi. First Realization of 3-Fold Fluxionality in Polycyclic Conjugated Hydrocarbon-Metal Complexes: Synthesis and Dynamic NMR Study of [Pd(.Eta.3-Phenalenyl)(Tmeda)]+PF6- and Its Methyl Derivative. *J. Am. Chem. Soc.* **1986**, *108* (2), 325–327. https://doi.org/10.1021/ja00262a039.

(8) Haddon, R. C.; Wudl, F.; Kaplan, M. L.; Marshall, J. H.; Cais, R. E.; Bramwell, F. B. 1,9-Dithiophenalenyl System. *J. Am. Chem. Soc.* **1978**, *100* (24), 7629–7633. https://doi.org/10.1021/ja00492a032.

(9) Goto, K.; Kubo, T.; Yamamoto, K.; Nakasuji, K.; Sato, K.; Shiomi, D.; Takui, T.; Kubota, M.; Kobayashi, T.; Yakusi, K.; Ouyang, J. A Stable Neutral Hydrocarbon Radical: Synthesis, Crystal Structure, and Physical Properties of 2,5,8-Tri- *Tert* -Butyl-Phenalenyl. *J. Am. Chem. Soc.* **1999**, *121* (7), 1619–1620. https://doi.org/10.1021/ja9836242.

(10) Suzuki, S.; Morita, Y.; Fukui, K.; Sato, K.; Shiomi, D.; Takui, T.; Nakasuji, K. Aromaticity on the Pancake-Bonded Dimer of Neutral Phenalenyl Radical as Studied by MS and NMR Spectroscopies and NICS Analysis. *J. Am. Chem. Soc.* **2006**, *128* (8), 2530–2531. https://doi.org/10.1021/ja058387z.

(11) Mota, F.; Miller, J. S.; Novoa, J. J. Comparative Analysis of the Multicenter, Long Bond in $[TCNE]^{\cdot-}$ and Phenalenyl Radical Dimers: A Unified Description of Multicenter, Long Bonds. *J. Am. Chem. Soc.* **2009**, *131* (22), 7699–7707. https://doi.org/10.1021/ja9002298.

(12) Morita, Y.; Aoki, T.; Fukui, K.; Nakazawa, S.; Tamaki, K.; Suzuki, S.; Fuyuhiro, A.; Yamamoto, K.; Sato, K.; Shiomi, D.; Naito, A.; Takui, T.; Nakasuji, K. A New Trend in Phenalenyl Chemistry: A Persistent Neutral Radical, 2,5,8-Tri-Tert-Butyl-1,3-Diazaphenalenyl, and the Excited Triplet State of the Gablesyn-Dimer in the Crystal of Column Motif. *Angew. Chem. Int. Ed.* **2002**, *41* (10), 1793–1796. https://doi.org/10.1002/1521-3773(20020517)41:10<1793::AID-ANIE1793>3.0.CO;2-G.

(13) Beer, L.; Mandal, S. K.; Reed, R. W.; Oakley, R. T.; Tham, F. S.; Donnadieu, B.; Haddon, R. C. The First Electronically Stabilized Phenalenyl Radical: Effect of Substituents on Solution Chemistry and Solid-State Structure. *Crystal Growth & Design* **2007**, *7* (4), 802–809. https://doi.org/10.1021/cg0603366.

(14) Morita, Y.; Ohba, T.; Haneda, N.; Maki, S.; Kawai, J.; Hatanaka, K.; Sato, K.; Shiomi, D.; Takui, T.; Nakasuji, K. New Persistent Radicals: Synthesis and Electronic Spin Structure of 2,5-Di- *Tert* -Butyl-6-Oxophenalenoxyl Derivatives. *J. Am. Chem. Soc.* **2000**, *122* (19), 4825–4826. https://doi.org/10.1021/ja000298t.

(15) Fukui, K.; Inoue, J.; Kubo, T.; Nakazawa, S.; Aoki, T.; Morita, Y.; Yamamoto, K.; Sato, K.; Shiomi, D.; Nakasuji, K.; Takui, T. The First Non-Kekulé Polynuclear Aromatic High-Spin Hydrocarbon: Generation of a Triangulene Derivative and Band Structure Calculation of Triangulene-Based High-Spin Hydrocarbons. *Synthetic Metals* **2001**, *121* (1–3), 1824–1825. https://doi.org/10.1016/S0379-6779(00)01023-7.

(16) Kubo, T.; Goto, Y.; Uruichi, M.; Yakushi, K.; Nakano, M.; Fuyuhiro, A.; Morita, Y.; Nakasuji, K. Synthesis and Characterization of Acetylene-Linked Bisphenalenyl and Metallic-Like Behavior in Its Charge-Transfer Complex. *Chem. Asian J.* **2007**, *2* (11), 1370–1379. https://doi.org/10.1002/asia.200700147.

(17) Yang, Y.; Blacque, O.; Sato, S.; Juríček, M. Cycloparaphenylene–Phenalenyl Radical and Its Dimeric Double Nanohoop**. *Angew Chem Int Ed* **2021**, *60* (24), 13529–13535. https://doi.org/10.1002/anie.202101792.

(18) Hirao, Y.; Daifuku, Y.; Ihara, K.; Kubo, T. Spin–Spin Interactions in One-Dimensional Assemblies of a Cumulene-Based Singlet Biradical. *Angewandte Chemie* **2021**, *133* (39), 21489–21496. https://doi.org/10.1002/ange.202105740.

(19) Ohta, S.; Nakano, M.; Kubo, T.; Kamada, K.; Ohta, K.; Kishi, R.; Nakagawa, N.; Champagne, B.; Botek, E.; Umezaki, S.; Takebe, A.; Takahashi, H.; Furukawa, S.; Morita, Y.; Nakasuji, K.; Yamaguchi, K. Second Hyperpolarizability of Phenalenyl Radical System Involving Acetylene π-Conjugated Bridge. *Chemical Physics Letters* **2006**, *420* (4–6), 432–437. https://doi.org/10.1016/j.cplett.2006.01.022.

(20) Kamada, K.; Ohta, K.; Kubo, T.; Shimizu, A.; Morita, Y.; Nakasuji, K.; Kishi, R.; Ohta, S.; Furukawa, S.; Takahashi, H.; Nakano, M. Strong Two-Photon Absorption of Singlet Diradical Hydrocarbons. *Angew. Chem. Int. Ed.* **2007**, *46* (19), 3544–3546. https://doi.org/10.1002/anie.200605061.
(21) Haddon, R. C. Design of Organic Metals and Superconductors. *Nature* **1975**, *256* (5516), 394–396. https://doi.org/10.1038/256394a0.
(22) Chi, X.; Itkis, M. E.; Kirschbaum, K.; Pinkerton, A. A.; Oakley, R. T.; Cordes, A. W.; Haddon, R. C. Dimeric Phenalenyl-Based Neutral Radical Molecular Conductors. *J. Am. Chem. Soc.* **2001**, *123* (17), 4041–4048. https://doi.org/10.1021/ja0039785.
(23) Itkis, M. E.; Chi, X.; Cordes, A. W.; Haddon, R. C. Magneto-Opto-Electronic Bistability in a Phenalenyl-Based Neutral Radical. *Science* **2002**, *296* (5572), 1443–1445. https://doi.org/10.1126/science.1071372.
(24) Nakasuji, K.; Yoshida, K.; Murata, I. Design and Synthesis of an Amphoteric Four-Stage Redox Hydrocarbon Bearing Phenalenyl Moieties. 1,2-Bis(Phenalen-1-Yliden)Ethane. *J. Am. Chem. Soc.* **1982**, *104* (5), 1432–1433. https://doi.org/10.1021/ja00369a051.
(25) Nakasuji, K.; Yoshida, K.; Murata, I. Design and Synthesis of a Highly Amphoteric Condensed Hydrocarbon with the Highest Reduction Potential. Pentaleno[1,2,3-Cd:4,5,6-c'd']Diphenalene. *J. Am. Chem. Soc.* **1983**, *105* (15), 5136–5137. https://doi.org/10.1021/ja00353a049.
(26) Ohashi, K.; Kubo, T.; Masui, T.; Yamamoto, K.; Nakasuji, K.; Takui, T.; Kai, Y.; Murata, I. 4,8,12,16-Tetra- *Tert* -Butyl- *s* -Indaceno[1,2,3- *Cd* :5,6,7- *c* ' *d* ']Diphenalene: A Four-Stage Amphoteric Redox System. *J. Am. Chem. Soc.* **1998**, *120* (9), 2018–2027. https://doi.org/10.1021/ja970961m.
(27) Kubo, T.; Yamamoto, K.; Nakasuji, K.; Takui, T.; Murata, I. Hexa-Tert-Butyltribenzodecacyclenyl: A Six-Stage Amphoteric Redox System. *Angew. Chem. Int. Ed. Engl.* **1996**, *35* (4), 439–441. https://doi.org/10.1002/anie.199604391.
(28) Nakasuji, K.; Yoshida, K.; Murata, I. Synthesis and Electrochemical Characteristic of 1, 2-Bis (Phenalen-1-Ylidene) Ethene. An Amphoteric Four-Stage Redox Hydrocarbon. *Chem. Lett.* **1982**, *11* (7), 969–970. https://doi.org/10.1246/cl.1982.969.
(29) Murata, I.; Sasaki, S.; Klabunde, K.-U.; Toyoda, J.; Nakasuji, K. Synthesis of a Highly Amphoterics-Indaceno[1,2,3-Cd:5,6,7-C'd']Diphenalene: Switching between Diatropism and Paratropism Due to Changes in Oxidation Level. *Angew. Chem. Int. Ed. Engl.* **1991**, *30* (2), 172–173. https://doi.org/10.1002/anie.199101721.
(30) Mukherjee, A.; Sau, S. C.; Mandal, S. K. Exploring Closed-Shell Cationic Phenalenyl: From Catalysis to Spin Electronics. *Acc. Chem. Res.* **2017**, *50* (7), 1679–1691. https://doi.org/10.1021/acs.accounts.7b00141.
(31) Ahmed, J.; Datta, P.; Das, A.; Jomy, S.; Mandal, S. K. Switching between Mono and Doubly Reduced Odd Alternant Hydrocarbon: Designing a Redox Catalyst. *Chem. Sci.* **2021**, *12* (8), 3039–3049. https://doi.org/10.1039/D0SC05972B.
(32) Ahmed, J.; Chakraborty, S.; Jose, A.; P, S.; Mandal, S. K. Integrating Organic Lewis Acid and Redox Catalysis: The Phenalenyl Cation in Dual Role. *J. Am. Chem. Soc.* **2018**, *140* (26), 8330–8339. https://doi.org/10.1021/jacs.8b04786.
(33) Ahmed, J.; P, S.; Vijaykumar, G.; Jose, A.; Raj, M.; Mandal, S. K. A New Face of Phenalenyl-Based Radicals in the Transition Metal-Free C–H Arylation of Heteroarenes at Room Temperature: Trapping the Radical Initiator via C–C σ-Bond Formation. *Chem. Sci.* **2017**, *8* (11), 7798–7806. https://doi.org/10.1039/C7SC02661G.
(34) Sil, S.; Santha Bhaskaran, A.; Chakraborty, S.; Singh, B.; Kuniyil, R.; Mandal, S. K. Reduced-Phenalenyl-Based Molecule as a Super Electron Donor for Radical-Mediated C–N Coupling Catalysis at Room Temperature. *J. Am. Chem. Soc.* **2022**, *144* (49), 22611–22621. https://doi.org/10.1021/jacs.2c09225.

(35) Sen, P. P.; Roy, S. R. Introducing Phenalenyl-Based Organic Lewis Acid as a Photocatalyst to Facilitate Oxidative Azolation of Unactivated Arenes. *Org. Lett.* **2023**, *25* (11), 1895–1900. https://doi.org/10.1021/acs.orglett.3c00409.
(36) Payne, M. M.; Odom, S. A.; Parkin, S. R.; Anthony, J. E. Stable, Crystalline Acenedithiophenes with up to Seven Linearly Fused Rings. *Org. Lett.* **2004**, *6* (19), 3325–3328. https://doi.org/10.1021/ol048686d.
(37) Payne, M. M.; Parkin, S. R.; Anthony, J. E. Functionalized Higher Acenes: Hexacene and Heptacene. *J. Am. Chem. Soc.* **2005**, *127* (22), 8028–8029. https://doi.org/10.1021/ja051798v.
(38) Kaur, I.; Stein, N. N.; Kopreski, R. P.; Miller, G. P. Exploiting Substituent Effects for the Synthesis of a Photooxidatively Resistant Heptacene Derivative. *J. Am. Chem. Soc.* **2009**, *131* (10), 3424–3425. https://doi.org/10.1021/ja808881x.
(39) Kaur, I.; Jazdzyk, M.; Stein, N. N.; Prusevich, P.; Miller, G. P. Design, Synthesis, and Characterization of a Persistent Nonacene Derivative. *J. Am. Chem. Soc.* **2010**, *132* (4), 1261–1263. https://doi.org/10.1021/ja9095472.
(40) Zhang, X.; Jiang, X.; Luo, J.; Chi, C.; Chen, H.; Wu, J. A Cruciform 6,6'-Dipentacenyl: Synthesis, Solid-State Packing and Applications in Thin-Film Transistors. *Chem. Eur. J.* **2010**, *16* (2), 464–468. https://doi.org/10.1002/chem.200902675.
(41) Li, J.; Zhang, K.; Zhang, X.; Huang, K.-W.; Chi, C.; Wu, J. *Meso* -Substituted Bisanthenes as Soluble and Stable Near-Infrared Dyes. *J. Org. Chem.* **2010**, *75* (3), 856–863. https://doi.org/10.1021/jo902413h.
(42) Zhang, K.; Huang, K.-W.; Li, J.; Luo, J.; Chi, C.; Wu, J. A Soluble and Stable Quinoidal Bisanthene with NIR Absorption and Amphoteric Redox Behavior. *Org. Lett.* **2009**, *11* (21), 4854–4857. https://doi.org/10.1021/ol902241u.
(43) Konishi, A.; Hirao, Y.; Nakano, M.; Shimizu, A.; Botek, E.; Champagne, B.; Shiomi, D.; Sato, K.; Takui, T.; Matsumoto, K.; Kurata, H.; Kubo, T. Synthesis and Characterization of Teranthene: A Singlet Biradical Polycyclic Aromatic Hydrocarbon Having Kekulé Structures. *J. Am. Chem. Soc.* **2010**, *132* (32), 11021–11023. https://doi.org/10.1021/ja1049737.
(44) Chase, D. T.; Rose, B. D.; McClintock, S. P.; Zakharov, L. N.; Haley, M. M. Indeno[1,2-b]Fluorenes: Fully Conjugated Antiaromatic Analogues of Acenes. *Angew. Chem. Int. Ed.* **2011**, *50* (5), 1127–1130. https://doi.org/10.1002/anie.201006312.
(45) Chase, D. T.; Fix, A. G.; Rose, B. D.; Weber, C. D.; Nobusue, S.; Stockwell, C. E.; Zakharov, L. N.; Lonergan, M. C.; Haley, M. M. Electron-Accepting 6,12-Diethynylindeno[1,2-b]Fluorenes: Synthesis, Crystal Structures, and Photophysical Properties. *Angew. Chem. Int. Ed.* **2011**, *50* (47), 11103–11106. https://doi.org/10.1002/anie.201104797.
(46) Chase, D. T.; Fix, A. G.; Kang, S. J.; Rose, B. D.; Weber, C. D.; Zhong, Y.; Zakharov, L. N.; Lonergan, M. C.; Nuckolls, C.; Haley, M. M. 6,12-Diarylindeno[1,2- *b*]Fluorenes: Syntheses, Photophysics, and Ambipolar OFETs. *J. Am. Chem. Soc.* **2012**, *134* (25), 10349–10352. https://doi.org/10.1021/ja303402p.
(47) Rose, B. D.; Vonnegut, C. L.; Zakharov, L. N.; Haley, M. M. Fluoreno[4,3- *c*]Fluorene: A Closed-Shell, Fully Conjugated Hydrocarbon. *Org. Lett.* **2012**, *14* (9), 2426–2429. https://doi.org/10.1021/ol300942z.
(48) Li, Y.; Heng, W.-K.; Lee, B. S.; Aratani, N.; Zafra, J. L.; Bao, N.; Lee, R.; Sung, Y. M.; Sun, Z.; Huang, K.-W.; Webster, R. D.; López Navarrete, J. T.; Kim, D.; Osuka, A.; Casado, J.; Ding, J.; Wu, J. Kinetically Blocked Stable Heptazethrene and Octazethrene: Closed-Shell or Open-Shell in the Ground State? *J. Am. Chem. Soc.* **2012**, *134* (36), 14913–14922. https://doi.org/10.1021/ja304618v.
(49) Zeng, Z.; Sung, Y. M.; Bao, N.; Tan, D.; Lee, R.; Zafra, J. L.; Lee, B. S.; Ishida, M.; Ding, J.; López Navarrete, J. T.; Li, Y.; Zeng, W.; Kim, D.; Huang, K.-W.; Webster, R. D.; Casado, J.; Wu, J. Stable Tetrabenzo-Chichibabin's Hydrocarbons: Tunable Ground State and Unusual Transition between

Their Closed-Shell and Open-Shell Resonance Forms. *J. Am. Chem. Soc.* **2012**, *134* (35), 14513–14525. https://doi.org/10.1021/ja3050579.

(50) Fix, A. G.; Deal, P. E.; Vonnegut, C. L.; Rose, B. D.; Zakharov, L. N.; Haley, M. M. Indeno[2,1- *c*]Fluorene: A New Electron-Accepting Scaffold for Organic Electronics. *Org. Lett.* **2013**, *15* (6), 1362–1365. https://doi.org/10.1021/ol400318z.

(51) Anamimoghadam, O.; Symes, M. D.; Busche, C.; Long, D.-L.; Caldwell, S. T.; Flors, C.; Nonell, S.; Cronin, L.; Bucher, G. Naphthoxanthenyl, a New Stable Phenalenyl Type Radical Stabilized by Electronic Effects. *Org. Lett.* **2013**, *15* (12), 2970–2973. https://doi.org/10.1021/ol401117g.

(52) Konishi, A.; Hirao, Y.; Matsumoto, K.; Kurata, H.; Kishi, R.; Shigeta, Y.; Nakano, M.; Tokunaga, K.; Kamada, K.; Kubo, T. Synthesis and Characterization of Quarteranthene: Elucidating the Characteristics of the Edge State of Graphene Nanoribbons at the Molecular Level. *J. Am. Chem. Soc.* **2013**, *135* (4), 1430–1437. https://doi.org/10.1021/ja309599m.

(53) Young, B. S.; Chase, D. T.; Marshall, J. L.; Vonnegut, C. L.; Zakharov, L. N.; Haley, M. M. Synthesis and Properties of Fully-Conjugated Indacenedithiophenes. *Chem. Sci.* **2014**, *5* (3), 1008–1014. https://doi.org/10.1039/C3SC53181C.

(54) Maekawa, T.; Ueno, H.; Segawa, Y.; Haley, M. M.; Itami, K. Synthesis of Open-Shell Ladder π-Systems by Catalytic C–H Annulation of Diarylacetylenes. *Chem. Sci.* **2016**, *7* (1), 650–654. https://doi.org/10.1039/C5SC03391H.

(55) Marshall, J. L.; O'Neal, N. J.; Zakharov, L. N.; Haley, M. M. Synthesis and Characterization of Two Unsymmetrical Indenofluorene Analogues: Benzo[5,6]- *s* -Indaceno[1,2- *b*]Thiophene and Benzo[5,6]- *s* -Indaceno[2,1- *b*]Thiophene. *J. Org. Chem.* **2016**, *81* (9), 3674–3680. https://doi.org/10.1021/acs.joc.6b00340.

(56) Marshall, J. L.; Uchida, K.; Frederickson, C. K.; Schütt, C.; Zeidell, A. M.; Goetz, K. P.; Finn, T. W.; Jarolimek, K.; Zakharov, L. N.; Risko, C.; Herges, R.; Jurchescu, O. D.; Haley, M. M. Indacenodibenzothiophenes: Synthesis, Optoelectronic Properties and Materials Applications of Molecules with Strong Antiaromatic Character. *Chem. Sci.* **2016**, *7* (8), 5547–5558. https://doi.org/10.1039/C6SC00950F.

(57) Reus, C.; Lechner, M. P.; Schulze, M.; Lungerich, D.; Diner, C.; Gruber, M.; Stryker, J. M.; Hampel, F.; Jux, N.; Tykwinski, R. R. Unexpected Michael Additions on the Way to 2.3,8.9-Dibenzanthanthrenes with Interesting Structural Properties. *Chem. Eur. J.* **2016**, *22* (27), 9097–9101. https://doi.org/10.1002/chem.201601435.

(58) Frederickson, C. K.; Zakharov, L. N.; Haley, M. M. Modulating Paratropicity Strength in Diareno-Fused Antiaromatics. *J. Am. Chem. Soc.* **2016**, *138* (51), 16827–16838. https://doi.org/10.1021/jacs.6b11397.

(59) Frederickson, C. K.; Rose, B. D.; Haley, M. M. Explorations of the Indenofluorenes and Expanded Quinoidal Analogues. *Acc. Chem. Res.* **2017**, *50* (4), 977–987. https://doi.org/10.1021/acs.accounts.7b00004.

(60) Petersen, J. F.; Frederickson, C. K.; Marshall, J. L.; Rudebusch, G. E.; Zakharov, L. N.; Hammerich, O.; Haley, M. M.; Nielsen, M. B. Expanded Indacene–Tetrathiafulvalene Scaffolds: Structural Implications for Redox Properties and Association Behavior. *Chem. Eur. J.* **2017**, *23* (53), 13120–13130. https://doi.org/10.1002/chem.201702347.

(61) Ribar, P.; Valenta, L.; Šolomek, T.; Juríček, M. Rules of Nucleophilic Additions to Zigzag Nanographene Diones**. *Angewandte Chemie* **2021**, *133* (24), 13633–13640. https://doi.org/10.1002/ange.202016437.

(62) Xiang, Q.; Guo, J.; Xu, J.; Ding, S.; Li, Z.; Li, G.; Phan, H.; Gu, Y.; Dang, Y.; Xu, Z.; Gong, Z.; Hu, W.; Zeng, Z.; Wu, J.; Sun, Z. Stable Olympicenyl Radicals and Their π-Dimers. *J. Am. Chem. Soc.* **2020**, *142* (25), 11022–11031. https://doi.org/10.1021/jacs.0c02287.

(63) Barker, J. E.; Frederickson, C. K.; Jones, M. H.; Zakharov, L. N.; Haley, M. M. Synthesis and Properties of Quinoidal Fluorenofluorenes. *Org. Lett.* **2017**, *19* (19), 5312–5315. https://doi.org/10.1021/acs.orglett.7b02605.
(64) Dressler, J. J.; Zhou, Z.; Marshall, J. L.; Kishi, R.; Takamuku, S.; Wei, Z.; Spisak, S. N.; Nakano, M.; Petrukhina, M. A.; Haley, M. M. Synthesis of the Unknown Indeno[1,2- *a*]Fluorene Regioisomer: Crystallographic Characterization of Its Dianion. *Angew. Chem. Int. Ed.* **2017**, *56* (48), 15363–15367. https://doi.org/10.1002/anie.201709282.
(65) Anamimoghadam, O.; Symes, M. D.; Long, D.-L.; Sproules, S.; Cronin, L.; Bucher, G. Electronically Stabilized Nonplanar Phenalenyl Radical and Its Planar Isomer. *J. Am. Chem. Soc.* **2015**, *137* (47), 14944–14951. https://doi.org/10.1021/jacs.5b07959.
(66) Barker, J. E.; Dressler, J. J.; Cárdenas Valdivia, A.; Kishi, R.; Strand, E. T.; Zakharov, L. N.; MacMillan, S. N.; Gómez-García, C. J.; Nakano, M.; Casado, J.; Haley, M. M. Molecule Isomerism Modulates the Diradical Properties of Stable Singlet Diradicaloids. *J. Am. Chem. Soc.* **2020**, *142* (3), 1548–1555. https://doi.org/10.1021/jacs.9b11898.
(67) Dressler, J. J.; Cárdenas Valdivia, A.; Kishi, R.; Rudebusch, G. E.; Ventura, A. M.; Chastain, B. E.; Gómez-García, C. J.; Zakharov, L. N.; Nakano, M.; Casado, J.; Haley, M. M. Diindenoanthracene Diradicaloids Enable Rational, Incremental Tuning of Their Singlet-Triplet Energy Gaps. *Chem* **2020**, *6* (6), 1353–1368. https://doi.org/10.1016/j.chempr.2020.02.010.
(68) Chen, Z. X.; Li, Y.; Huang, F. Persistent and Stable Organic Radicals: Design, Synthesis, and Applications. *Chem* **2021**, *7* (2), 288–332. https://doi.org/10.1016/j.chempr.2020.09.024.
(69) Dressler, J. J.; Barker, J. E.; Karas, L. J.; Hashimoto, H. E.; Kishi, R.; Zakharov, L. N.; MacMillan, S. N.; Gomez-Garcia, C. J.; Nakano, M.; Wu, J. I.; Haley, M. M. Late-Stage Modification of Electronic Properties of Antiaromatic and Diradicaloid Indeno[1,2- *b*]Fluorene Analogues via Sulfur Oxidation. *J. Org. Chem.* **2020**, *85* (16), 10846–10857. https://doi.org/10.1021/acs.joc.0c01387.
(70) Xu, T.; Han, Y.; Shen, Z.; Hou, X.; Jiang, Q.; Zeng, W.; Ng, P. W.; Chi, C. Antiaromatic Dicyclopenta[*b,g*]/[*a,f*]Naphthalene Isomers Showing an Open-Shell Singlet Ground State with Tunable Diradical Character. *J. Am. Chem. Soc.* **2021**, *143* (49), 20562–20568. https://doi.org/10.1021/jacs.1c06677.
(71) Warren, G. I.; Barker, J. E.; Zakharov, L. N.; Haley, M. M. Enhancing the Antiaromaticity of *s* -Indacene through Naphthothiophene Fusion. *Org. Lett.* **2021**, *23* (13), 5012–5017. https://doi.org/10.1021/acs.orglett.1c01514.
(72) Barker, J. E.; Price, T. W.; Karas, L. J.; Kishi, R.; MacMillan, S. N.; Zakharov, L. N.; Gómez-García, C. J.; Wu, J. I.; Nakano, M.; Haley, M. M. A Tale of Two Isomers: Enhanced Antiaromaticity/Diradical Character versus Deleterious Ring-Opening of Benzofuran-fused *s* -Indacenes and Dicyclopenta[*b* , *g*]Naphthalenes. *Angew Chem Int Ed* **2021**, *60* (41), 22385–22392. https://doi.org/10.1002/anie.202107855.
(73) Wehrmann, C. M.; Charlton, R. T.; Chen, M. S. A Concise Synthetic Strategy for Accessing Ambient Stable Bisphenalenyls toward Achieving Electroactive Open-Shell π-Conjugated Materials. *J. Am. Chem. Soc.* **2019**, *141* (7), 3240–3248. https://doi.org/10.1021/jacs.8b13300.
(74) Jousselin-Oba, T.; Mamada, M.; Marrot, J.; Maignan, A.; Adachi, C.; Yassar, A.; Frigoli, M. Excellent Semiconductors Based on Tetracenotetracene and Pentacenopentacene: From Stable Closed-Shell to Singlet Open-Shell. *J. Am. Chem. Soc.* **2019**, *141* (23), 9373–9381. https://doi.org/10.1021/jacs.9b03488.
(75) Jousselin-Oba, T.; Deal, P. E.; Fix, A. G.; Frederickson, C. K.; Vonnegut, C. L.; Yassar, A.; Zakharov, L. N.; Frigoli, M.; Haley, M. M. Synthesis and Properties of Benzo-Fused Indeno[2,1- *c*]Fluorenes. *Chem. Asian J.* **2019**, *14* (10), 1737–1744. https://doi.org/10.1002/asia.201801684.
(76) Jousselin-Oba, T.; Mamada, M.; Okazawa, A.; Marrot, J.; Ishida, T.; Adachi, C.; Yassar, A.; Frigoli, M. Modulating the Ground State, Stability and Charge Transport in OFETs of Biradicaloid Hexahydro-

Diindenopyrene Derivatives and a Proposed Method to Estimate the Biradical Character. *Chem. Sci.* **2020**, *11* (44), 12194–12205. https://doi.org/10.1039/D0SC04583G.

(77) Zong, C.; Yang, S.; Sun, Y.; Zhang, L.; Hu, J.; Hu, W.; Li, R.; Sun, Z. Isomeric Dibenzooctazethrene Diradicals for High-Performance Air-Stable Organic Field-Effect Transistors. *Chem. Sci.* **2022**, *13* (38), 11442–11447. https://doi.org/10.1039/D2SC03667C.

(78) Guo, Y.; Ding, S.; Zhang, N.; Xu, Z.; Wu, S.; Hu, J.; Xiang, Q.; Li, Z.-Y.; Chen, X.; Sato, S.; Wu, J.; Sun, Z. π-Extended Doublet Open-Shell Graphene Fragments Exhibiting One-Dimensional Chain Stacking. *J. Am. Chem. Soc.* **2022**, *144* (5), 2095–2100. https://doi.org/10.1021/jacs.1c12854.

(79) Jousselin-Oba, T.; Mamada, M.; Wright, K.; Marrot, J.; Adachi, C.; Yassar, A.; Frigoli, M. Synthesis, Aromaticity, and Application of *Peri* -Pentacenopentacene: Localized Representation of Benzenoid Aromatic Compounds. *Angewandte Chemie Intl Edit* **2022**, *61* (1). https://doi.org/10.1002/anie.202112794.

(80) Anthony, J. E.; Brooks, J. S.; Eaton, D. L.; Parkin, S. R. Functionalized Pentacene: Improved Electronic Properties from Control of Solid-State Order. *J. Am. Chem. Soc.* **2001**, *123* (38), 9482–9483. https://doi.org/10.1021/ja0162459.

(81) Arikawa, S.; Shimizu, A.; Shiomi, D.; Sato, K.; Shintani, R. Synthesis and Isolation of a Kinetically Stabilized Crystalline Triangulene. *J. Am. Chem. Soc.* **2021**, *143* (46), 19599–19605. https://doi.org/10.1021/jacs.1c10151.

(82) Kuriakose, F.; Commodore, M.; Hu, C.; Fabiano, C. J.; Sen, D.; Li, R. R.; Bisht, S.; Üngör, Ö.; Lin, X.; Strouse, G. F.; DePrince, A. E.; Lazenby, R. A.; Mentink-Vigier, F.; Shatruk, M.; Alabugin, I. V. Design and Synthesis of Kekulè and Non-Kekulè Diradicaloids via the Radical Periannulation Strategy: The Power of Seven Clar's Sextets. *J. Am. Chem. Soc.* **2022**, *144* (51), 23448–23464. https://doi.org/10.1021/jacs.2c09637.

(83) Tsvetkov, N. P.; Gonzalez-Rodriguez, E.; Hughes, A.; dos Passos Gomes, G.; White, F. D.; Kuriakose, F.; Alabugin, I. V. Radical Alkyne *Peri* -Annulation Reactions for the Synthesis of Functionalized Phenalenes, Benzanthrenes, and Olympicene. *Angew. Chem. Int. Ed.* **2018**, *57* (14), 3651–3655. https://doi.org/10.1002/anie.201712783.

(84) Hoye, T. R.; Baire, B.; Niu, D.; Willoughby, P. H.; Woods, B. P. The Hexadehydro-Diels–Alder Reaction. *Nature* **2012**, *490* (7419), 208–212. https://doi.org/10.1038/nature11518.

(85) Chernick, E. T.; Tykwinski, R. R. Carbon-Rich Nanostructures: The Conversion of Acetylenes into Materials: The Conversion of Acetylenes into Materials. *J. Phys. Org. Chem.* **2013**, *26* (9), 742–749. https://doi.org/10.1002/poc.3160.

(86) Hein, S. J.; Lehnherr, D.; Arslan, H.; J. Uribe-Romo, F.; Dichtel, W. R. Alkyne Benzannulation Reactions for the Synthesis of Novel Aromatic Architectures. *Acc. Chem. Res.* **2017**, *50* (11), 2776–2788. https://doi.org/10.1021/acs.accounts.7b00385.

(87) Ozaki, K.; Murai, K.; Matsuoka, W.; Kawasumi, K.; Ito, H.; Itami, K. One-Step Annulative π-Extension of Alkynes with Dibenzosiloles or Dibenzogermoles by Palladium/ *o* -chloranil Catalysis. *Angew. Chem. Int. Ed.* **2017**, *56* (5), 1361–1364. https://doi.org/10.1002/anie.201610374.

(88) Senese, A.; Chalifoux, W. Nanographene and Graphene Nanoribbon Synthesis via Alkyne Benzannulations. *Molecules* **2018**, *24* (1), 118. https://doi.org/10.3390/molecules24010118.

(89) Alabugin, I. V.; Gonzalez-Rodriguez, E. Alkyne Origami: Folding Oligoalkynes into Polyaromatics. *Acc. Chem. Res.* **2018**, *51* (5), 1206–1219. https://doi.org/10.1021/acs.accounts.8b00026.

(90) Stará, I. G.; Starý, I. Helically Chiral Aromatics: The Synthesis of Helicenes by [2 + 2 + 2] Cycloisomerization of π-Electron Systems. *Acc. Chem. Res.* **2020**, *53* (1), 144–158. https://doi.org/10.1021/acs.accounts.9b00364.

(91) Bergman, H. M.; Kiel, G. R.; Handford, R. C.; Liu, Y.; Tilley, T. D. Scalable, Divergent Synthesis of a High Aspect Ratio Carbon Nanobelt. *J. Am. Chem. Soc.* **2021**, *143* (23), 8619–8624. https://doi.org/10.1021/jacs.1c04037.

(92) Chen, Q.; Thoms, S.; Stöttinger, S.; Schollmeyer, D.; Müllen, K.; Narita, A.; Basché, T. Dibenzo[*Hi* , *St*]Ovalene as Highly Luminescent Nanographene: Efficient Synthesis via Photochemical Cyclodehydroiodination, Optoelectronic Properties, and Single-Molecule Spectroscopy. *J. Am. Chem. Soc.* **2019**, *141* (41), 16439–16449. https://doi.org/10.1021/jacs.9b08320.

(93) Yin, X.; Zheng, K.; Jin, Z.; Horst, M.; Xia, Y. Synthesis of Contorted Polycyclic Conjugated Hydrocarbons via Regioselective Activation of Cyclobutadienoids. *J. Am. Chem. Soc.* **2022**, *144* (28), 12715–12724. https://doi.org/10.1021/jacs.2c02457.

(94) Mohamed, R. K.; Mondal, S.; Guerrera, J. V.; Eaton, T. M.; Albrecht-Schmitt, T. E.; Shatruk, M.; Alabugin, I. V. Alkynes as Linchpins for the Additive Annulation of Biphenyls: Convergent Construction of Functionalized Fused Helicenes. *Angew. Chem. Int. Ed.* **2016**, *55* (39), 12054–12058. https://doi.org/10.1002/anie.201606330.

(95) von Kugelgen, S.; Piskun, I.; Griffin, J. H.; Eckdahl, C. T.; Jarenwattananon, N. N.; Fischer, F. R. Templated Synthesis of End-Functionalized Graphene Nanoribbons through Living Ring-Opening Alkyne Metathesis Polymerization. *J. Am. Chem. Soc.* **2019**, *141* (28), 11050–11058. https://doi.org/10.1021/jacs.9b01805.

(96) Kawade, R. K.; Hu, C.; Dos Santos, N. R.; Watson, N.; Lin, X.; Hanson, K.; Alabugin, I. V. Phenalenannulations: Three-Point Double Annulation Reactions That Convert Benzenes into Pyrenes. *Angew. Chem. Int. Ed.* **2020**, *59* (34), 14352–14357. https://doi.org/10.1002/anie.202006087.

(97) Hu, C.; Mena, J.; Alabugin, I. V. Design Principles of the Use of Alkynes in Radical Cascades. *Nat Rev Chem* **2023**. https://doi.org/10.1038/s41570-023-00479-w.

(98) Gonzalez-Rodriguez, E.; Abdo, M. A.; dos Passos Gomes, G.; Ayad, S.; White, F. D.; Tsvetkov, N. P.; Hanson, K.; Alabugin, I. V. Twofold π-Extension of Polyarenes via Double and Triple Radical Alkyne *Peri* -Annulations: Radical Cascades Converging on the Same Aromatic Core. *J. Am. Chem. Soc.* **2020**, *142* (18), 8352–8366. https://doi.org/10.1021/jacs.0c01856.

(99) Park, J. H.; Liu, T.; Kim, K. C.; Lee, S. W.; Jang, S. S. Systematic Molecular Design of Ketone Derivatives of Aromatic Molecules for Lithium-Ion Batteries: First-Principles DFT Modeling. *ChemSusChem* **2017**, *10* (7), 1584–1591. https://doi.org/10.1002/cssc.201601730.

(100) Alabugin, I. V.; Kuhn, L.; Medvedev, M. G.; Krivoshchapov, N. V.; Vil', V. A.; Yaremenko, I. A.; Mehaffy, P.; Yarie, M.; Terent'ev, A. O.; Zolfigol, M. A. Stereoelectronic Power of Oxygen in Control of Chemical Reactivity: The Anomeric Effect Is Not Alone. *Chem. Soc. Rev.* **2021**, *50* (18), 10253–10345. https://doi.org/10.1039/D1CS00386K.

(101) Kochi, J. K. Chemistry of Alkoxy Radicals: Cleavage Reactions. *J. Am. Chem. Soc.* **1962**, *84* (7), 1193–1197. https://doi.org/10.1021/ja00866a026.

(102) Tappin, N. D. C.; Renaud, P. Methyl Radical Initiated Kharasch and Related Reactions. *Adv. Synth. Catal.* **2021**, *363* (1), 275–282. https://doi.org/10.1002/adsc.202001000.

(103) Zhang, K.; Chang, L.; An, Q.; Wang, X.; Zuo, Z. Dehydroxymethylation of Alcohols Enabled by Cerium Photocatalysis. *J. Am. Chem. Soc.* **2019**, *141* (26), 10556–10564. https://doi.org/10.1021/jacs.9b05932.

(104) Hu, A.; Chen, Y.; Guo, J.-J.; Yu, N.; An, Q.; Zuo, Z. Cerium-Catalyzed Formal Cycloaddition of Cycloalkanols with Alkenes through Dual Photoexcitation. *J. Am. Chem. Soc.* **2018**, *140* (42), 13580–13585. https://doi.org/10.1021/jacs.8b08781.

(105) Kariofillis, S. K.; Jiang, S.; Żurański, A. M.; Gandhi, S. S.; Martinez Alvarado, J. I.; Doyle, A. G. Using Data Science To Guide Aryl Bromide Substrate Scope Analysis in a Ni/Photoredox-Catalyzed Cross-Coupling with Acetals as Alcohol-Derived Radical Sources. *J. Am. Chem. Soc.* **2022**, *144* (2), 1045–1055. https://doi.org/10.1021/jacs.1c12203.

(106) Olson, A. S.; Jameson, A. J.; Kyasa, S. K.; Evans, B. W.; Dussault, P. H. Reductive Cleavage of Organic Peroxides by Iron Salts and Thiols. *ACS Omega* **2018**, *3* (10), 14054–14063. https://doi.org/10.1021/acsomega.8b01977.
(107) dos Passos Gomes, G.; Wimmer, A.; Smith, J. M.; König, B.; Alabugin, I. V. CO_2 or SO_2 : Should It Stay, or Should It Go? *J. Org. Chem.* **2019**, *84* (10), 6232–6243. https://doi.org/10.1021/acs.joc.9b00503.
(108) Kariofillis, S. K.; Doyle, A. G. Synthetic and Mechanistic Implications of Chlorine Photoelimination in Nickel/Photoredox C(Sp^3)–H Cross-Coupling. *Acc. Chem. Res.* **2021**, *54* (4), 988–1000. https://doi.org/10.1021/acs.accounts.0c00694.
(109) Ohno, A.; Kito, N.; Ohnishi, Y. Thermal and Photolytic Decompositions of Azobis(2-Phenoxy)-2-Propane. *BCSJ* **1971**, *44* (2), 467–470. https://doi.org/10.1246/bcsj.44.467.
(110) Harris, T.; Gomes, G. dos P.; Clark, R. J.; Alabugin, I. V. Domino Fragmentations in Traceless Directing Groups of Radical Cascades: Evidence for the Formation of Alkoxy Radicals via C–O Scission. *J. Org. Chem.* **2016**, *81* (14), 6007–6017. https://doi.org/10.1021/acs.joc.6b01052.
(111) Matsuoka, T.; Inuki, S.; Miyagawa, T.; Oishi, S.; Ohno, H. Total Synthesis of (+)-Polyoxamic Acid via Visible-Light-Mediated Photocatalytic β-Scission and 1,5-Hydrogen Atom Transfer of Glucose Derivative. *J. Org. Chem.* **2020**, *85* (12), 8271–8278. https://doi.org/10.1021/acs.joc.0c00910.
(112) Berkowitz, A. J.; Murelli, R. P. Synthesis of α-Tropolones through Autoxidation of Dioxole-Fused Cycloheptatrienes. *J. Org. Chem.* **2022**, *87* (7), 4499–4507. https://doi.org/10.1021/acs.joc.1c02713.
(113) El Gehani, A. A. M. A.; Maashi, H. A.; Harnedy, J.; Morrill, L. C. Electrochemical Generation and Utilization of Alkoxy Radicals. *Chem. Commun.* **2023**, 10.1039.D3CC00302G. https://doi.org/10.1039/D3CC00302G.
(114) Brás, E. M.; Cabral, L. I. L.; Amado, P. S. M.; Abe, M.; Fausto, R.; Cristiano, M. L. S. Photoinduced Reactivity in a Dispiro-1,2,4-Trioxolane: Adamantane Ring Expansion and First Direct Observation of the Long-Lived Triplet Diradical Intermediates. *J. Phys. Chem. A* **2020**, *124* (21), 4202–4210. https://doi.org/10.1021/acs.jpca.0c01974.
(115) Abe, M.; Inakazu, T.; Munakata, J.; Nojima, M. ^{18}O-Tracer Studies of Fe(II)-Induced Decomposition of 1,2,4-Trioxolanes (Ozonides) Derived from Cyclopentenes and Indenes. Inner-Sphere Electron Transfer Reduction of the Peroxide Linkage. *J. Am. Chem. Soc.* **1999**, *121* (28), 6556–6562. https://doi.org/10.1021/ja990807v.
(116) Coote, M. L.; Easton, C. J.; Zard, S. Z. Factors Affecting the Relative and Absolute Rates of β-Scission of Alkoxythiocarbonyl Radicals and Alkoxycarbonyl Radicals. *J. Org. Chem.* **2006**, *71* (13), 4996–4999. https://doi.org/10.1021/jo0607313.
(117) Barton, D. H. R.; McCombie, S. W. A New Method for the Deoxygenation of Secondary Alcohols. *J. Chem. Soc., Perkin Trans. 1* **1975**, No. 16, 1574. https://doi.org/10.1039/p19750001574.
(118) Baroudi, A.; Alicea, J.; Flack, P.; Kirincich, J.; Alabugin, I. V. Radical O→C Transposition: A Metal-Free Process for Conversion of Phenols into Benzoates and Benzamides. *J. Org. Chem.* **2011**, *76* (6), 1521–1537. https://doi.org/10.1021/jo102467j.
(119) Baroudi, A.; Mauldin, J.; Alabugin, I. V. Conformationally Gated Fragmentations and Rearrangements Promoted by Interception of the Bergman Cyclization through Intramolecular H-Abstraction: A Possible Mechanism of Auto-Resistance to Natural Enediyne Antibiotics? *J. Am. Chem. Soc.* **2010**, *132* (3), 967–979. https://doi.org/10.1021/ja905100u.
(120) Dong, Z.; MacMillan, D. W. C. Metallaphotoredox-Enabled Deoxygenative Arylation of Alcohols. *Nature* **2021**, *598* (7881), 451–456. https://doi.org/10.1038/s41586-021-03920-6.
(121) Sakai, H. A.; MacMillan, D. W. C. Nontraditional Fragment Couplings of Alcohols and Carboxylic Acids: C(Sp^3)–C(Sp^3) Cross-Coupling via Radical Sorting. *J. Am. Chem. Soc.* **2022**, *144* (14), 6185–6192. https://doi.org/10.1021/jacs.2c02062.

(122) Kariofillis, S. K.; Shields, B. J.; Tekle-Smith, M. A.; Zacuto, M. J.; Doyle, A. G. Nickel/Photoredox-Catalyzed Methylation of (Hetero)Aryl Chlorides Using Trimethyl Orthoformate as a Methyl Radical Source. *J. Am. Chem. Soc.* **2020**, *142* (16), 7683–7689. https://doi.org/10.1021/jacs.0c02805.
(123) Capaldo, L.; Ravelli, D. Alkoxy Radicals Generation: Facile Photocatalytic Reduction of N-Alkoxyazinium or Azolium Salts. *Chem. Commun.* **2019**, *55* (21), 3029–3032. https://doi.org/10.1039/C9CC00035F.
(124) Chang, L.; An, Q.; Duan, L.; Feng, K.; Zuo, Z. Alkoxy Radicals See the Light: New Paradigms of Photochemical Synthesis. *Chem. Rev.* **2022**, *122* (2), 2429–2486. https://doi.org/10.1021/acs.chemrev.1c00256.
(125) Budnikov, A. S.; Krylov, I. B.; Lastovko, A. V.; Yu, B.; Terent'ev, A. O. N-Alkoxyphtalimides as Versatile Alkoxy Radical Precursors in Modern Organic Synthesis. *Asian Journal of Organic Chemistry* **2022**, *11* (8), e202200262. https://doi.org/10.1002/ajoc.202200262.
(126) Wu, X.; Zhu, C. Recent Advances in Ring-Opening Functionalization of Cycloalkanols by C-C σ-Bond Cleavage. *Chem. Rec.* **2018**, *18* (6), 587–598. https://doi.org/10.1002/tcr.201700090.
(127) Shi, J.-L.; Wang, Y.; Wang, Z.; Dou, B.; Wang, J. Ring-Opening Iodination and Bromination of Unstrained Cycloalkanols through β-Scission of Alkoxy Radicals. *Chem. Commun.* **2020**, *56* (37), 5002–5005. https://doi.org/10.1039/D0CC01720E.
(128) Bailey, W. J. Free Radical Ring-Opening Polymerization. *Polym J* **1985**, *17* (1), 85–95. https://doi.org/10.1295/polymj.17.85.
(129) Tardy, A.; Nicolas, J.; Gigmes, D.; Lefay, C.; Guillaneuf, Y. Radical Ring-Opening Polymerization: Scope, Limitations, and Application to (Bio)Degradable Materials. *Chem. Rev.* **2017**, *117* (3), 1319–1406. https://doi.org/10.1021/acs.chemrev.6b00319.
(130) Curran, D. P. The Design and Application of Free Radical Chain Reactions in Organic Synthesis. Part 1. *Synthesis* **1988**, *1988* (06), 417–439. https://doi.org/10.1055/s-1988-27600.
(131) Curran, D. P. The Design and Application of Free Radical Chain Reactions in Organic Synthesis. Part 2. *Synthesis* **1988**, *1988* (07), 489–513. https://doi.org/10.1055/s-1988-27620.
(132) Elliott, Q.; Alabugin, I. V. AIBN as an Electrophilic Reagent for Cyano Group Transfer. *J. Org. Chem.* **2023**, *88* (4), 2648–2654. https://doi.org/10.1021/acs.joc.2c02859.
(133) Alabugin, I. V.; Gilmore, K.; Patil, S.; Manoharan, M.; Kovalenko, S. V.; Clark, R. J.; Ghiviriga, I. Radical Cascade Transformations of Tris(*o* -Aryleneethynylenes) into Substituted Benzo[*a*]Indeno[2,1- *c*]Fluorenes. *J. Am. Chem. Soc.* **2008**, *130* (34), 11535–11545. https://doi.org/10.1021/ja8038213.
(134) Byers, P. M.; Rashid, J. I.; Mohamed, R. K.; Alabugin, I. V. Polyaromatic Ribbon/Benzofuran Fusion via Consecutive Endo Cyclizations of Enediynes. *Org. Lett.* **2012**, *14* (23), 6032–6035. https://doi.org/10.1021/ol302922t.
(135) Zhou, Z.; Egger, D. T.; Hu, C.; Pennachio, M.; Wei, Z.; Kawade, R. K.; Üngör, Ö.; Gershoni-Poranne, R.; Petrukhina, M. A.; Alabugin, I. V. Localized Antiaromaticity Hotspot Drives Reductive Dehydrogenative Cyclizations in Bis- and Mono-Helicenes. *J. Am. Chem. Soc.* **2022**, *144* (27), 12321–12338. https://doi.org/10.1021/jacs.2c03681.
(136) Zhou, Z.; Kawade, R. K.; Wei, Z.; Kuriakose, F.; Üngör, Ö.; Jo, M.; Shatruk, M.; Gershoni-Poranne, R.; Petrukhina, M. A.; Alabugin, I. V. Negative Charge as a Lens for Concentrating Antiaromaticity: Using a Pentagonal "Defect" and Helicene Strain for Cyclizations. *Angewandte Chemie Intl Edit* **2020**, *59* (3), 1256–1262. https://doi.org/10.1002/anie.201911319.
(137) Pati, K.; dos Passos Gomes, G.; Harris, T.; Hughes, A.; Phan, H.; Banerjee, T.; Hanson, K.; Alabugin, I. V. Traceless Directing Groups in Radical Cascades: From Oligoalkynes to Fused Helicenes without Tethered Initiators. *J. Am. Chem. Soc.* **2015**, *137* (3), 1165–1180. https://doi.org/10.1021/ja510563d.
(138) Hughes, A. M.; dos Passos Gomes, G.; Alabugin, I. V. Stereoelectronic Influence of a "Spectator" Propargylic Substituent Can Override Aromaticity Effects in Radical *Peri* -Cyclizations En Route to

Expanded Polyaromatics. *J. Org. Chem.* **2019**, *84* (4), 1853–1862. https://doi.org/10.1021/acs.joc.8b02779.
(139) Pati, K.; dos Passos Gomes, G.; Alabugin, I. V. Combining Traceless Directing Groups with Hybridization Control of Radical Reactivity: From Skipped Enynes to Defect-Free Hexagonal Frameworks. *Angew. Chem.* **2016**, *128* (38), 11805–11809. https://doi.org/10.1002/ange.201605799.
(140) Mondal, S.; Mohamed, R. K.; Manoharan, M.; Phan, H.; Alabugin, I. V. Drawing from a Pool of Radicals for the Design of Selective Enyne Cyclizations. *Org. Lett.* **2013**, *15* (22), 5650–5653. https://doi.org/10.1021/ol4028072.
(141) Mondal, S.; Gold, B.; Mohamed, R. K.; Alabugin, I. V. Design of Leaving Groups in Radical C□C Fragmentations: Through-Bond 2c-3e Interactions in Self-Terminating Radical Cascades. *Chem. Eur. J.* **2014**, *20* (28), 8664–8669. https://doi.org/10.1002/chem.201402843.
(142) Mohamed, R. K.; Mondal, S.; Gold, B.; Evoniuk, C. J.; Banerjee, T.; Hanson, K.; Alabugin, I. V. Alkenes as Alkyne Equivalents in Radical Cascades Terminated by Fragmentations: Overcoming Stereoelectronic Restrictions on Ring Expansions for the Preparation of Expanded Polyaromatics. *J. Am. Chem. Soc.* **2015**, *137* (19), 6335–6349. https://doi.org/10.1021/jacs.5b02373.
(143) Beckwith, A. L. J.; Bowry, V. W.; Bowman, W. R.; Mann, E.; Parr, J.; Storey, J. M. D. The Mechanism of Bu_3SnH-Mediated Homolytic Aromatic Substitution. *Angew Chem Int Ed* **2004**, *43* (1), 95–98. https://doi.org/10.1002/anie.200352419.
(144) Reetz, M. T. Dyotropic Rearrangements, a New Class of Orbital-Symmetry Controlled Reactions. Type I. *Angew. Chem. Int. Ed. Engl.* **1972**, *11* (2), 129–130. https://doi.org/10.1002/anie.197201291.
(145) Fernández, I.; Cossío, F. P.; Sierra, M. A. Dyotropic Reactions: Mechanisms and Synthetic Applications. *Chem. Rev.* **2009**, *109* (12), 6687–6711. https://doi.org/10.1021/cr900209c.
(146) Davis, R. L.; Tantillo, D. J. Dissecting a Dyotropic Rearrangement. *J. Org. Chem.* **2010**, *75* (5), 1693–1700. https://doi.org/10.1021/jo902685x.
(147) Croisant, M. F.; Van Hoveln, R.; Schomaker, J. M. Formal Dyotropic Rearrangements in Organometallic Transformations: Formal Dyotropic Rearrangements in Organometallic Transformations. *Eur. J. Org. Chem.* **2015**, *2015* (27), 5897–5907. https://doi.org/10.1002/ejoc.201500561.
(148) Gridnev, I. Sigmatropic and Haptotropic Rearrangements in Organometallic Chemistry. *Coordination Chemistry Reviews* **2008**, *252* (15–17), 1798–1818. https://doi.org/10.1016/j.ccr.2007.10.021.
(149) Fernández, I.; Sierra, M. A.; Cossío, F. P. Stereoelectronic Effects on Type I 1,2-Dyotropic Rearrangements in Vicinal Dibromides. *Chem. Eur. J.* **2006**, *12* (24), 6323–6330. https://doi.org/10.1002/chem.200501517.
(150) Gibian, M. J.; Corley, R. C. Organic Radical-Radical Reactions. Disproportionation vs. Combination. *Chem. Rev.* **1973**, *73* (5), 441–464. https://doi.org/10.1021/cr60285a002.
(151) Shen, D.; Pritchard, H. O. On the Dynamics of Free-Radical Disproportionation Reactions. *Theoret. Chim. Acta* **1991**, *78* (4), 241–246. https://doi.org/10.1007/BF01112847.
(152) An, Q.; Xing, Y.-Y.; Pu, R.; Jia, M.; Chen, Y.; Hu, A.; Zhang, S.-Q.; Yu, N.; Du, J.; Zhang, Y.; Chen, J.; Liu, W.; Hong, X.; Zuo, Z. Identification of Alkoxy Radicals as Hydrogen Atom Transfer Agents in Ce-Catalyzed C–H Functionalization. *J. Am. Chem. Soc.* **2023**, *145* (1), 359–376. https://doi.org/10.1021/jacs.2c10126.
(153) Chamulitrat, W.; Jordan, S. J.; Mason, R. P. Fatty Acid Radical Formation in Rats Administered Oxidized Fatty Acids: In Vivo Spin Trapping Investigation. *Archives of Biochemistry and Biophysics* **1992**, *299* (2), 361–367. https://doi.org/10.1016/0003-9861(92)90288-8.
(154) Dikalov, S.; Kirilyuk, I.; Grigor'ev, I. Spin Trapping of O-, C-, and S-Centered Radicals and Peroxynitrite by 2H-Imidazole-1-Oxides. *Biochemical and Biophysical Research Communications* **1996**, *218* (2), 616–622. https://doi.org/10.1006/bbrc.1996.0109.

(155) Kalyanaraman, B.; Karoui, H.; Singh, R. J.; Felix, C. C. Detection of Thiyl Radical Adducts Formed during Hydroxyl Radical- and Peroxynitrite-Mediated Oxidation of Thiols—A High Resolution ESR Spin-Trapping Study at Q-Band (35 GHz). *Analytical Biochemistry* **1996**, *241* (1), 75–81. https://doi.org/10.1006/abio.1996.0380.

(156) Eckhardt, P.; Elliot, Q.; Alabugin, I. V.; Opatz, T. Two Paths to Oxidative C−H Amination Under Basic Conditions: A Theoretical Case Study Reveals Hidden Opportunities Provided by Electron Upconversion**. *Chemistry A European J* **2022**, *28* (60), e202201637. https://doi.org/10.1002/chem.202201637.

(157) De Vleeschouwer, F.; Van Speybroeck, V.; Waroquier, M.; Geerlings, P.; De Proft, F. Electrophilicity and Nucleophilicity Index for Radicals. *Org. Lett.* **2007**, *9* (14), 2721–2724. https://doi.org/10.1021/ol071038k.

(158) Kailass, K.; Sadovski, O.; Capello, M.; Kang, Y.; Fleming, J. B.; Hanash, S. M.; Beharry, A. A. Measuring Human Carboxylesterase 2 Activity in Pancreatic Cancer Patient-Derived Xenografts Using a Ratiometric Fluorescent Chemosensor. *Chem. Sci.* **2019**, *10* (36), 8428–8437. https://doi.org/10.1039/C9SC00283A.

(159) Kuo, C.; Rao, N. S.; Patil, P. B.; Chiang, T.; Kavala, V.; Yao, C. Synthesis of Perinaphthenones *via* $BF_3 \cdot Et_2O$ Mediated One-Pot Cascade 4,5-Annulation Reactions of 1-Naphthols and Ynones. *Adv. Synth. Catal.* **2021**, *363* (7), 1935–1943. https://doi.org/10.1002/adsc.202001558.

(160) Schmidt, R.; Tanielian, C.; Dunsbach, R.; Wolff, C. Phenalenone, a Universal Reference Compound for the Determination of Quantum Yields of Singlet Oxygen O2(1Δg) Sensitization. *Journal of Photochemistry and Photobiology A: Chemistry* **1994**, *79* (1–2), 11–17. https://doi.org/10.1016/1010-6030(93)03746-4.

(161) Oliveros, E.; Bossmann, S. H.; Nonell, S.; Martí, C.; Heit, G.; Tröscher, G.; Neuner, A.; Martínez, C.; Braun, A. M. Photochemistry of the Singlet Oxygen [O2(1Δg)] Sensitizer Perinaphthenone (Phenalenone) in N,N′-Dimethylacetamide and 1,4-Dioxane. *New J. Chem.* **1999**, *23* (1), 85–93. https://doi.org/10.1039/a804054k.

(162) Martí, C.; Jürgens, O.; Cuenca, O.; Casals, M.; Nonell, S. Aromatic Ketones as Standards for Singlet Molecular Oxygen Photosensitization. Time-Resolved Photoacoustic and near-IR Emission Studies. *Journal of Photochemistry and Photobiology A: Chemistry* **1996**, *97* (1–2), 11–18. https://doi.org/10.1016/1010-6030(96)04321-3.

(163) Segado, M.; Reguero, M. Mechanism of the Photochemical Process of Singlet Oxygen Production by Phenalenone. *Phys. Chem. Chem. Phys.* **2011**, *13* (9), 4138. https://doi.org/10.1039/c0cp01827a.

(164) Espinoza, C.; Trigos, Á.; Medina, M. E. Theoretical Study on the Photosensitizer Mechanism of Phenalenone in Aqueous and Lipid Media. *J. Phys. Chem. A* **2016**, *120* (31), 6103–6110. https://doi.org/10.1021/acs.jpca.6b03615.

(165) Song, R.; Feng, Y.; Wang, D.; Xu, Z.; Li, Z.; Shao, X. Phytoalexin Phenalenone Derivatives Inactivate Mosquito Larvae and Root-Knot Nematode as Type-II Photosensitizer. *Sci Rep* **2017**, *7* (1), 42058. https://doi.org/10.1038/srep42058.

(166) Casellas, J.; Reguero, M. Photosensitization Versus Photocyclization: Competitive Reactions of Phenylphenalenone in Its Role as Phytoanticipins in Plant Defense Strategies. *J. Phys. Chem. A* **2018**, *122* (3), 811–821. https://doi.org/10.1021/acs.jpca.7b11569.

(167) Godard, J.; Brégier, F.; Arnoux, P.; Myrzakhmetov, B.; Champavier, Y.; Frochot, C.; Sol, V. New Phenalenone Derivatives: Synthesis and Evaluation of Their Singlet Oxygen Quantum Yield. *ACS Omega* **2020**, *5* (43), 28264–28272. https://doi.org/10.1021/acsomega.0c04172.

(168) Marzooghi, S.; Di Toro, D. M. A Critical Review of Polycyclic Aromatic Hydrocarbon Phototoxicity Models: Critical Review of PAH Phototoxicity Models. *Environ Toxicol Chem* **2017**, *36* (5), 1138–1148. https://doi.org/10.1002/etc.3722.

(169) Nathusius, M.; Ejlli, B.; Rominger, F.; Freudenberg, J.; Bunz, U. H. F.; Müllen, K. Chrysene-Based Blue Emitters. *Chem. Eur. J.* **2020**, *26* (66), 15089–15093. https://doi.org/10.1002/chem.202001808.
(170) Frisch, M. J. T.; Schlegel, H. B.; Scuseria, G. E.; Robb, M. A.; Cheeseman, J. R.; Scalmani, G.; Barone, V.; Mennucci, B.; Petersson, G. A.; Nakatsuji, H.; Caricato, M.; Li, X.; Hratchian, H. P.; Izmaylov, A. F.; Bloino, J.; Zheng, G.; Sonnenberg, J. L.; Hada, M.; Ehara, M.; Toyota, K.; Fukuda, R.; Hasegawa, J.; Ishida, M.; Nakajima, T.; Honda, Y.; Kitao, O.; Nakai, H.; Vreven, T.; Montgomery, J. A., Jr; Peralta, J. E.; Ogliaro, F.; Bearpark, M.; Heyd, J. J.; Brothers, E.; Kudin, K. N.; Staroverov, V. N.; Kobayashi, R.; Normand, J.; Raghavachari, K.; Rendell, A.; Burant, J. C.; Iyengar, S. S.; Tomasi, J.; Cossi, M.; Rega, N.; Millam, J. M.; Klene, M.; Knox, J. E.; Cross, J. B.; Bakken, V.; Adamo, C.; Jaramillo, J.; Gomperts, R.; Stratmann, R. E.; Yazyev, O.; Austin, A. J.; Cammi, R.; Pomelli, C.; Ochterski, J. W.; Martin, R. L.; Morokuma, K.; Zakrzewski, V. G.; Voth, G. A.; Salvador, P.; Dannenberg, J. J.; Dapprich, S.; Daniels, A. D.; Farkas, O.; Foresman, J. B.; Ortiz, J. V.; Cioslowski, J.; Fox, D. J. Gaussian 09, 2009.
(171) Grimme, S.; Bannwarth, C.; Shushkov, P. A Robust and Accurate Tight-Binding Quantum Chemical Method for Structures, Vibrational Frequencies, and Noncovalent Interactions of Large Molecular Systems Parametrized for All Spd-Block Elements (*Z* = 1–86). *J. Chem. Theory Comput.* **2017**, *13* (5), 1989–2009. https://doi.org/10.1021/acs.jctc.7b00118.
(172) Zhao, Y.; Truhlar, D. G. The M06 Suite of Density Functionals for Main Group Thermochemistry, Thermochemical Kinetics, Noncovalent Interactions, Excited States, and Transition Elements: Two New Functionals and Systematic Testing of Four M06 Functionals and 12 Other Functionals. *Theor Chem Account* **2008**, *119* (5–6), 525–525. https://doi.org/10.1007/s00214-007-0401-8.
(173) Zhao, Y.; Truhlar, D. G. Density Functionals with Broad Applicability in Chemistry. *Acc. Chem. Res.* **2008**, *41* (2), 157–167. https://doi.org/10.1021/ar700111a.
(174) Zhao, Y.; Truhlar, D. G. How Well Can New-Generation Density Functionals Describe the Energetics of Bond-Dissociation Reactions Producing Radicals? *J. Phys. Chem. A* **2008**, *112* (6), 1095–1099. https://doi.org/10.1021/jp7109127.
(175) Pracht, P.; Bohle, F.; Grimme, S. Automated Exploration of the Low-Energy Chemical Space with Fast Quantum Chemical Methods. *Phys. Chem. Chem. Phys.* **2020**, *22* (14), 7169–7192. https://doi.org/10.1039/C9CP06869D.
(176) Gilbert, A. IQmol Molecular. http://iqmol.org/ (accessed 2023-03-10).
(177) Legault, C. CYLview, 2009. https://www.cylview.org/ (accessed 2023-03-10).

TOC abstract: